LLaMP: LARGE LANGUAGE MODEL MADE POWERFUL FOR HIGH-FIDELITY MATERIALS KNOWLEDGE RETRIEVAL

Yuan Chiang[1,2*†], **Elvis Hsieh**[1*], **Chia-Hong Chou**[3], **Janosh Riebesell**[2,4]
[1]University of California, Berkeley, [2]Lawrence Berkeley National Laboratory,
[3]Foothill College, [4]Cavendish Laboratory, University of Cambridge, UK

ABSTRACT

Materials science research requires multi-step reasoning and precise material informatics retrieval, where minor errors can propagate into significant failures in downstream experiments. Despite their general success, Large Language Models (LLMs) often struggle with hallucinations, handling domain-specific data effectively (e.g., crystal structures), and integrating experimental workflows. To address these challenges, we introduce LLaMP, a hierarchical multi-agent framework designed to emulate the materials science research workflow. The high-level supervisor agent decomposes user requests into sub-tasks and coordinates with specialized assistant agents. These assistant agents handle domain-specific tasks, such as retrieving and processing data from the Materials Project (MP) or conducting simulations as needed. This pipeline facilitates iterative refinement of material property predictions and enables the simulation of real-world research workflows. To ensure reliability, we propose a novel metric combining uncertainty and confidence estimates to evaluate the self-consistency of responses from LLaMP and other methods. Our experiments with real-world materials science tasks demonstrate LLaMP's superior performance in material property prediction, crystal structure editing, and annealing molecular dynamics simulations using pre-trained interatomic potentials. Unlike prior work focused solely on material property prediction or discovery, LLaMP serves as a foundation for autonomous materials research by combining grounded informatics and enabling iterative experimental processes.

1 INTRODUCTION

The generation of convincing yet unreliable information poses a pressing challenge to large language model (LLMs), particularly to their application in the sciences. LLMs are prone to hallucination–providing false information with high confidence (Xu et al., 2024; Bang et al., 2023). This issue is particularly concerning for knowledge-intensive tasks, where users rely on chatbots and other AI systems to provide accurate guidance (Lewis et al., 2020). LLMs often lack up-to-date factual knowledge on topics outside their training data, requiring rigorous verification against trusted external sources (Mallen et al., 2023). In the scientific community, where the integration of insights and data accuracy is already complex, the proliferation of generative models may exacerbate the risk of misinformation. This trend accentuates the importance of scrutinizing and ensuring the reliability of information sources.

Current approaches to enhance LLM accuracy in domain-specific knowledge often involve fine-tuning pre-trained models (Gupta et al., 2022; Dagdelen et al., 2024) or tailored prompt engineering techniques (Yang et al., 2023; Zheng et al., 2023). While these models are easy to deploy, they suffer from diminished reproducibility and data adherence due to the absence of a memory base, and untraceable fine-tuning history. Even though fine-tuning can encode a certain amount of domain-specific knowledge into LLMs, it is constrained by scalability and intrinsic memory capac-

*Equal Contribution.
†Correspondence to: cyrusyc@berkeley.edu

ity. Fine-tuned LLMs struggle to retain in the long term the knowledge they were trained on as the training progresses, nor can they be aware of the recent events and data beyond pre-training. Prompt engineering, while effective, also compromises the generalizability, thus limiting the overall power and flexibility of LLMs. Therefore, a more sensible approach involves equipping LLMs with external data sources, allowing them to generate holistic responses via few-shot adaptation to factual information (Lewis et al., 2021) that can reliably support real-world scientific research and decision-making.

In this work, we propose LLaMP, a hierarchical multi-agent framework that leverages reasoning-and-acting (ReAct) (Yao et al., 2023) agents with Materials Project (MP), arXiv, Wikipedia, and atomistic simulation tools. The framework serves as a safeguard against LLM hallucination by grounding them in high-fidelity material informatics from large-scale material database, including computational data from quantum-mechanical first-principles calculations and expert-curated material synthesis recipes, and further enables the capabilities of complex downstream tasks. The hierarchical planning of supervisor and assistant agents improves tool-usage performance and enhances consistency in final responses with self-correcting mechanism. LLaMP supports a wide range of advanced capabilities, including multi-modal searching, tensor and 3D crystal structure retrieval and operation, and language-driven simulation. The framework not only can accurately retrieve high-fidelity, higher-order materials data but also can combine different modalities to perform complex, knowledge-intensive inferences and operations essential for real-world materials science applications.

Our contributions are as follows: (1) we introduce a hierarchical agentic framework that enables LLMs to access high-fidelity materials informatics and perform complex simulation; (2) we propose a statistical metric to assess the self-consistency of LLM responses in high-precision, reproducibility-critical settings; (3) we evaluate the performance of LLaMP and standard LLMs in predicting material properties, including bulk moduli, electronic bandgaps, formation energies, and magnetic orderings; (4) we demonstrate real-world applications in materials science, including inorganic synthesis, crystal structure generation and editing, and high-throughput atomistic simulations using pre-trained force fields, highlighting the potential of language-driven experimentation for automating and accelerating scientific discovery.

2 Related Work

Materials science databases and benchmarks The Materials Project is a multi-institution effort to explore and compute the properties of all known inorganic materials (Jain et al., 2013) and molecules (Spotte-Smith et al., 2023). The initiative leverages high-throughput electronic structure calculations (Kresse & Furthmüller, 1996; Shao et al., 2015) based on density functional theory (DFT), providing large-scale open-source database and analysis algorithms, with the goal to drastically reduce the time and cost required for materials discovery by focusing experiments on the promising candidates from computational screening. Most of the atomic structures are selected from the Inorganic Crystal Structure Database (ICSD) (Zagorac et al., 2019) and undergo standardized relaxation procedures, followed by post-processing or additional calculations for higher-order material properties such as electron and phonon bandgaps, elastic tensors, and dielectric tensors. Complementing MP, the Automatic FLOW for Materials Discovery (AFLOW) provides a database of over 3.5 million compounds and extensive computational tools (Curtarolo et al., 2012a), while the Open Quantum Materials Database (OQMD) focuses on thermodynamic and structural properties (Kirklin et al., 2015a), and the Novel Materials Discovery (NOMAD) Laboratory offers a FAIR-compliant platform for managing and sharing materials science data (Scheidgen et al., 2023b). Despite the value of these resources, MP distinguishes itself with its curated, high-fidelity dataset, which is continuously updated and vetted by the community, ensuring reliability and scientific validity for downstream applications.

Prompting and fine-tuning LLM in science domain Prompt-based methods have been used as effective tools for automating the data extraction process from the literature. (Polak & Morgan, 2023) employ a prompt workflow to extract the cooling rates of metallic glasses and yield strengths of high entropy alloys. (Zheng et al., 2023) implement a ChatGPT metal-organic framework (MOF) synthesis assistant through embedding and searching on preselected papers. StructChem (Ouyang et al., 2024) leverages step-by-step reasoning and iteratively refines results to solve college-level

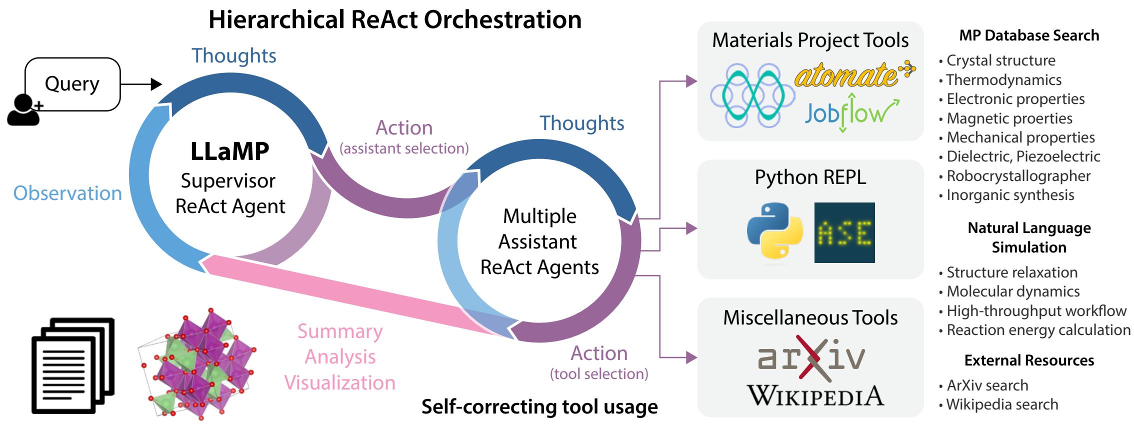

Figure 1: Hierarchical multi-agent planning in LLaMP. Designed to emulate the materials science research workflow, LLaMP employs a two-level agentic structure, Supervisor ReAct agent decomposes user queries into sub-tasks and oversees multiple specialized assistant agents. These assistants retrieve high-fidelity data from the Materials Project (MP) and perform domain-specific tasks like crystal structure manipulation and molecular dynamics simulations. For a detailed example, refer to Figure A.1.

chemistry questions. Yang et al. (2023) use GPT-4 to extract experimentally measured bandgaps to train a graph neural network for accurate bandgap prediction from crystal structures. Other works address the challenges of extracting complex materials informatics from diverse formats such as tables and unstructured texts (Hira et al., 2024; Schilling-Wilhelmi et al., 2024). Despite the success in the specific data extraction tasks, prompt-based methods face challenges in reproducibility when the used prompts are fine-grained to work for specific edge cases. They are also still prone to hallucination and less generalizable to combine different data sources due to the deliberately designed prompt.

Several other knowledge-grounded, domain-specific language models lean on the fine-tuning approach against pre-selected data and literature. For instance, ChemGPT (Frey et al., 2022) involves fine-tuning GPT-neo on self-referencing embedded strings (SELFIES) representations of small molecules. Jablonka et al. (2024) demonstrated GPT-3 fine-tuned against online corpora could outperform purpose-trained models on classification, regression, and inverse design of high-entropy alloys and molecules. Dagdelen et al. (2024) fine-tuned GPT-3 on $\sim$500 prompt-completion pairs to enhance LLM's capability to extract useful information on materials chemistry from text paragraphs. Cha et al. (2024) further curated instruction data to fine-tune Llama for material science-specific tasks. Xie et al. (2023) combines question-answering fine-tuning with multi-task learning. However, the fine-tuned models without augmentation inherently lack awareness of the up-to-date results, and any data is only available after their training. Furthermore, these works focus on general (undergraduate-level) question answering (Zaki et al., 2023; Song et al., 2023; Wang et al., 2023) instead of factual grounding on expert-curated database and downstream experimental workflow.

LLM agent and tool usage An emerging class of LLM applications take advantage of LLM text completion and instruction following capability for function calling. This approach extends LLMs with expert-curated tools to improve the quality of control for downstream applications (Chase, 2022; Qin et al., 2023; Wang et al., 2024; Shinn et al., 2023; Du et al., 2024; Lu et al., 2024). In the science domain, such an approach is widely adopted. Coscientist (Boiko et al., 2023) combines tools such as search engines, Python, and document index for autonomous chemical research. ChemCrow (M. Bran et al., 2024) gathers multiple molecule and safety tools to enhance organic chemistry experiments and molecule design. Ghafarollahi & Buehler (2024) propose AtomAgents for alloy design and analysis. Concurrently, Zhang et al. (2024) develop a retrieval-based agent on their curated dataset. However, most prior works adopt the flat planning strategy, where a single agent accesses all the available tools, resulting in a lack of self-correcting and iterative refinement capabilities. We mitigate this through hierarchical structure of multi-agents (see Section 3).

3 METHOD

3.1 HIERARCHICAL MULTI-AGENT PLANNING

Overview Flat planning, where a single agent sees all the available tools and related API schemas, quickly exceeds the context window and incurs a huge cost for multimodal data processing in material science. To manage heterogeneous data sources and diverse queries, we introduce hierarchical multi-agent planning, featuring a supervisor agent overseeing multiple specialized assistant agents (Figure 1). Two levels of agents are deployed using a standardized LangChain interface (Chase, 2022). This design offers three major advantages over flat planning commonly implemented in previous works (Boiko et al., 2023; M. Bran et al., 2024): (1) modularity of the system ensures that each assistant agent can focus on domain-specific queries while the supervisor agent handles higher-level reasoning and task allocation; (2) the hierarchical structure improves the overall accuracy and efficiency by minimizing the context window consumption and schema parsing; (3) the multi-agent collaboration allows the iterative refinement on multimodal data (Figure A.1) and long-horizon simulation (Appendix C).

Supervisor agent The supervisor agent acts as a router and decision-maker, handling abstract logic between user requests and assistant agents. Here, we adopt ReAct (Yao et al., 2023) on GPT-4 to augment the agent's action space $\mathcal{A}$ with a language space $\mathcal{L}$ to create an expanded action space of $\hat{\mathcal{A}} = \mathcal{A} \cup \mathcal{L}$. Instead of executing a direct function call, the supervisor dynamically delegates queries to assistant agents via natural language, ensuring a human-interpretable reasoning trace. This approach enhances contextual grounding, ensuring that factual information and numerically accurate simulations. By modularizing factual grounding and simulation tasks, the supervisor effectively reduces error propagation where reasoning errors in materials properties compound across multiple steps.

Assistant agent One of the critical failures in the scientific domain (Miret & Krishnan, 2024) is the LLM-generated hallucinations and incorrect outputs that mislead downstream experiments. To mitigate this, each MP assistant agent directly retrieves materials informatics from the Materials Project, ensuring grounded reasoning with expert-verified data.

Under the modular architecture, we assign a specialized ReAct agent for each specific tool or API endpoint. It reduces context window consumption, as each agent handles only the relevant schema for its task, avoiding unnecessary schema parsing. Additionally, the assistant agents can refine their API calls based on feedback, significantly improving task completion rates through the iterative self-correcting mechanism.

The full list of agents and tools are defined in A.2. Each MP assistant agent employs a self-correcting mechanism, enabling agents to refine their API calls and improve task completion rates. The framework's modularity enables seamless integration of new assistant agents, allowing for extensibility to various materials discovery methods and experimental techniques (Zeni et al., 2024; Luo et al., 2023; Pilania et al., 2017; Wen et al., 2024; 2023)

3.2 SELF-CONSISTENCY OF RESPONSE (SCOR)

When LLMs are integrated into scientific workflows and deployed in high-stakes settings (*i.e.* self-driving labs), it is important for these models to have consistent and predictable behaviors (Liang et al., 2023). For numeric knowledge retrieval tasks, we define the following metrics:

Precision (sample standard deviation) measures the uncertainty in the model's responses where n is the number of valid responses from N trials and $\hat{\sigma}$ is the standard deviation of a valid response:

$$\text{Precision} = \frac{\hat{\sigma}}{\sqrt{n}} \geq 0$$

.

Coefficient of Precision (CoP) maps the precision to $(0, 1]$:

$$\text{CoP} = \exp\left(-\text{Precision}\right) = \exp\left(-\frac{\hat{\sigma}}{\sqrt{n}}\right) \in (0, 1] \,.$$

Confidence measures the ratio of generating n valid responses in N trials:

$$\text{Confidence} = \frac{n}{N}.$$

Self-consistency of Response (SCoR) is then defined as

$$\text{SCoR} = \text{CoP} \times \text{Confidence} \in [0, 1] .$$

The limit of SCoR $= 1$ is reached when the model yields the same response to a given query every time. At the limit of SCoR $= 0$, the model is either very inconsistent (with large variance across the responses) or very reluctant (with low confidence) to answer the query. Despite the simplicity in definition, SCoR effectively reflects the reproducibility and practical usability of the method, which is important when the method is incorporated into broader systems where the stable and expected behaviors are prioritized. Detailed metric calculation can be found in Appendix A.3.

4 Experiments

	Bulk Modulus K (GPa)					Formation Energy ΔH_f (eV)				
	Precision↓	CoP	Confidence	SCoR↑	MAE↓	Precision↓	CoP	Confidence	SCoR↑	MAE↓
LLaMP (GPT-4)	2.698	0.900	1.000	0.900	**14.574**	0.006	0.994	0.940	0.934	0.007
LLaMP (Sonnet)	1.816	0.562	1.000	0.562	15.104	0.000	1.000	1.000	**1.000**	**0.000**
LLaMP (Gemini)	5.178	0.053	1.000	0.053	16.251	0.076	0.932	0.620	0.576	0.166
LLaMP (Llama3)	12.993	0.036	0.800	0.029	50.308	0.000	1.000	0.250	0.250	1.377
HoneyBee	54.105	0.010	0.900	0.010	110.151	0.132	0.881	0.440	0.430	1.518
StructChem	0.000	1.000	0.200	0.200	41.017	0.000	1.000	0.200	0.200	3.146
Darwin	0.001	0.999	0.500	0.499	156.266	0.003	0.997	1.000	0.997	2.245
GPT-4+Serp	2.221	0.833	0.300	0.433	29.937	0.025	0.977	0.560	0.791	11.669
GPT-4	0.186	0.910	1.000	0.910	41.225	0.000	1.000	0.180	0.200	1.680
Sonnet	0.009	0.992	1.000	**0.992**	41.033	0.022	0.979	1.000	0.979	294.360
Gemini-Pro	6.065	0.169	1.000	0.169	43.429	0.467	0.657	1.000	0.657	1.412
Llama 3	11.222	0.010	1.000	0.010	41.874	2.346	0.139	0.960	0.137	4.657

	Electronic Bandgap E_g - Common (eV)					Electronic Bandgap E_g - Multi-element (eV)				
	Precision↓	CoP	Confidence	SCoR↑	MAE↓	Precision↓	CoP	Confidence	SCoR↑	MAE↓
LLaMP (GPT-4)	0.000	1.000	0.800	0.800	**0.000**	0.047	0.958	0.960	0.918	**0.167**
LLaMP (Sonnet)	0.145	0.870	0.600	0.522	0.298	0.046	0.962	1.000	0.962	0.304
LLaMP (Gemini)	0.627	0.571	0.600	0.343	1.327	0.003	0.997	0.500	0.997	0.637
LLaMP (Llama3)	0.051	0.952	0.800	0.761	1.038	0.169	0.848	0.800	0.678	1.094
HoneyBee	0.249	0.800	1.000	0.800	1.242	0.299	0.779	0.740	0.601	1.640
StructChem	0.017	0.984	1.000	0.984	0.986	0.000	1.000	0.200	0.200	0.973
Darwin	0.002	0.998	1.000	0.998	1.224	0.000	1.000	1.000	**1.000**	1.951
GPT-4+Serp	0.040	0.963	1.000	0.963	1.012	0.000	1.000	0.660	0.660	0.576
GPT-4	0.032	0.970	1.000	0.970	0.959	-	-	0.000	0.000	-
Sonnet	0.000	1.000	1.000	**1.000**	0.938	0.000	1.000	0.500	1.000	0.644
Gemini-Pro	0.034	0.968	1.000	0.968	0.994	0.168	0.849	0.600	0.509	0.989
Llama 3	0.042	0.960	1.000	0.960	1.053	0.182	0.836	0.860	0.719	1.091

Table 1: Performance metrics of LLaMP and baselines on material properties prediction tasks. The metrics from left to right are precision (sample standard deviation), coefficient of precision (CoP), confidence, self-consistency of response (SCoR), and mean absolute error (MAE), with theoretical values computed in the Materials Project taken as the ground truth. All the values are the average metrics over five runs and the sampled materials. Better method has high SCoR and MAE simultaneously. Full values across five runs are provided in Figure A.2

4.1 Material Properties Prediction

Response quality and consistency The prior benchmarks in materials science often focus on graduate school-level question-answering datasets (Wang et al., 2023; Zaki et al., 2023) or are limited to a single data modality (Rubungo et al., 2024). These approaches overlook the complexity of materials science, which involves reasoning across multiple properties and modalities. To bridge this gap, we benchmark material property prediction on bulk modulus, formation energy, and bandgap for both common and multi-element materials. We consider four baselines: StructChem with GPT-4 (prompting-based) (Ouyang et al., 2024), Darwin (fine-tuned) (Xie et al., 2023), HoneyBee (fine-tuned) (Cha et al., 2024), GPT-4 with search engine tool (RAG), and vanilla LLMs (`gpt-4, llama3-8b, gemini-1.0-pro`). Performance is assessed through Precision, CoP, SCoR, and MAE metrics, as defined in Section 3.2. We argue that any useful LLM agents to be included in the scientific workflow should have high SCoR and low error on the material's properties. Notably, LLaMP consistently outperforms other models, achieving the highest SCoR and the lowest errors across material properties, making it highly suitable for scientific workflows. Despite employing extensive prompting strategies, StructChem struggles due to its lack of domain-specific knowledge, leading to frequent refusals when it cannot verify outputs. Similarly, GPT-4 with SerpAPI suffers from noisy and inconsistent web sources, which degrade precision.

For bulk modulus prediction, vanilla LLMs, particularly Llama 3-8b, frequently rely on low-fidelity online data, leading to significant deviations for elements like Cr, Mn, and Fe, compared to MP theoretical values. Interestingly, Llama 3-8b usually cites spurious references in the responses despite the largest response variance but occasionally agrees with MP values. In contrast, LLaMP outperforms vanilla LLMs and reduces the MAE from around 40 to 14.57 GPa.

For formation energy prediction, vanilla LLMs suffer from low SCoR and high MAE ranging from 1.5 to 5.5 eV, which is impractical for material discovery requiring meV-level precision. This is not unexpected, since accurate formation energy prediction requires the computation of multiple energetics (energies of the compound itself and its elemental constituents).

For bandgaps prediction, we query 10 common compounds and 10 multi-element materials that are less commonly encountered in the literature. Vanilla LLMs perform surprisingly well on the bandgaps of common semiconductors (Table 1), with expected systematic deviation from MP values retrieved by LLaMP[1]. This is likely due to the extensive literature on experimental semiconductor bandgaps, which have been studied and reported for decades. On the contrary, vanilla LLMs lack intrinsic knowledge of the bandgaps for the queried multi-element materials and exhibit low confidence or refuse to make predictions (Table 1, Table B6.8), whereas LLaMP retrieves accurate data with a SCoR of 0.938 and correctly identifies the stable polymorph's bandgap when multiple forms are present.

Ablation study Our ablation study evaluates the impact of factual grounding and function-calling capabilities on LLaMP's performance. In Table 1, we examine three variants: (1) LLaMP; (2) GPT-4+ReAct with SerpAPI for internet browsing; (3) vanilla GPT-4. LLaMP achieved the best performance when using the complete set of MP tools, highlighting the importance of grounding in up-to-date, high-fidelity materials databases. In Section 3, we mentioned the importance of hierarchical planning for robust function calls. Evaluating several backbone models on bulk moduli, formation energy prediction, and bandgap, we found LLaMP's grounding performance correlates with the function-calling capability of backbone LLM: Claude-3.5-Sonnet (#1) $>$ Gemini-1.5-Flash (#24) $>$ and Llama3-8B (#46). The number following each model refers to its ranking on the Berkeley Function-Calling Leaderboard at the time of the experiment (Yan et al., 2024). These results highlight LLaMP's robust adaptability across different LLM backbones, demonstrating that it's hierarchical multi-agent planning consistently enhances performance and scale with the function-calling capability.

High-fidelity and higher-order data retrieval To assess LLaMP's effectiveness in handling large-scale, complex material properties, we randomly selected 800 unary, binary, and ternary compounds from the Materials Project (MP). We then evaluated LLaMP, GPT-3.5, and GPT-4 on magnetic ordering classification and total magnetization prediction, tasks that are inherently challenging due to the subtle distinctions between magnetic orderings and magnetization units. Our result indicates that vanilla LLMs suffer from hallucinations and misclassify the magnetic orderings of materials. LLaMP with GPT-4 as backend counteracts the intrinsic bias of GPT models, increasing the classification accuracy to 0.98 and R^2 of magnetization prediction to 0.992 (Table 2). We note that GPT-3.5 as backend struggles to distinguish `total_magnetization` from `magnetization_per_formula_unit` in magnetism API schema and often requests the wrong field and forgets to normalize the values. In the magnetic orderings queries, LLaMP with GPT-3.5 as backend fails to distinguish ferromagnetic (FM) and ferrimagnetic (FiM) orderings, while LLaMP with GPT-4 as backend gracefully separates the two classes (Figure 2a, d).

[1]Bandgaps calculated from generalized gradient approximation (GGA) functional are known to underestimate the experimental values by 40-50% (Borlido et al., 2020). Strategies to improve bandgap prediction at moderate or low computational cost will be included in MP in the future.

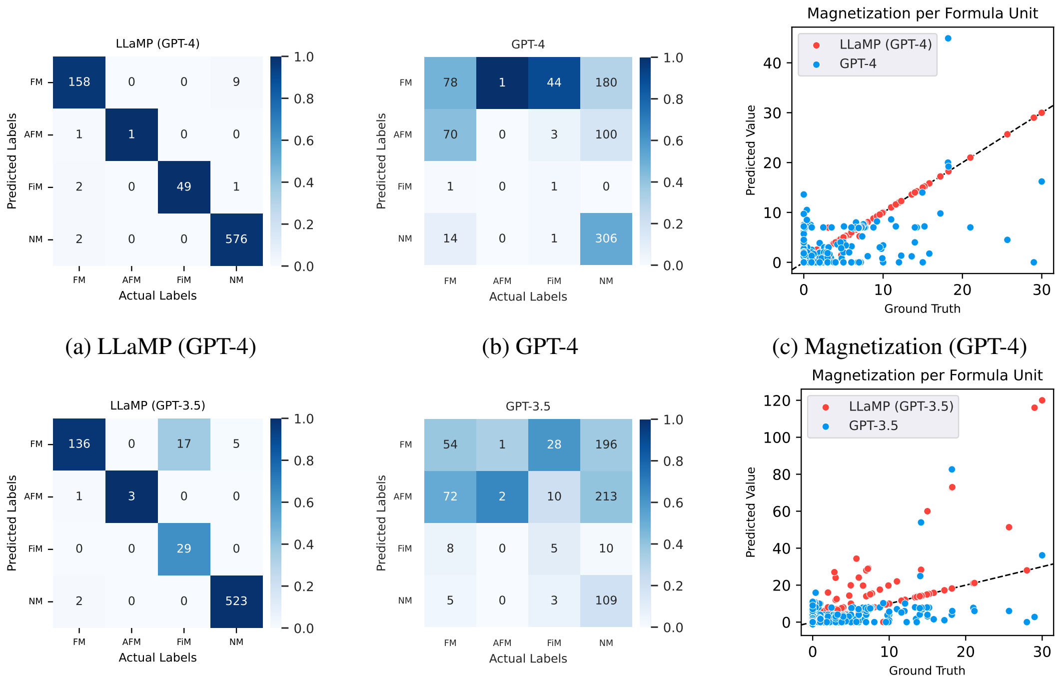

(a) LLaMP (GPT-4) (b) GPT-4 (c) Magnetization (GPT-4)

(d) LLaMP (GPT-3.5) (e) GPT-3.5 (f) Magnetization (GPT-3.5)

Figure 2: Prediction of LLaMP, GPT-3.5, and GPT-4 on (a,b,d,e) magnetic orderings and (c,f) total magnetization per formula unit of randomly selected materials. Confusion matrix presents the number of entries in each class. Colormap represents the percentage of correct classification.

4.2 Real-World Applications

Inorganic synthesis recipes Equipped with the MP synthesis endpoint (Kononova et al., 2019), LLaMP can extract synthesis recipes and summarize detailed step-by-step procedures grounded on real experimental papers with associated DOI references, as demonstrated in the example queries (Table B6.9 and B6.10).

Table 2: Prediction performance of LLaMP, GPT-3.5, and GPT-4 on magnetic orderings and magnetization. LLaMP with GPT-4 and GPT-3.5 as backend LLM are compared.

	Magnetic Ordering		Magnetization	
	Accuracy	F1	MAE	R^2
LLaMP (GPT-4)	**0.98**	**0.89**	**0.045**	**0.992**
GPT-4	0.48	0.26	1.611	-0.201
LLaMP (GPT-3.5)	0.96	0.88	1.896	0.407
GPT-3.5	0.23	0.18	1.988	-0.024

Vanilla LLMs often give seemingly correct and verbose synthesis procedures but pull irrelevant compounds into the recipes and overlook more optimal or efficient reactions. In the example of $YMnO_3$ (Table B6.9), GPT-3.5 suggests the possible reaction pathways from two common oxide precursors (Y_2O_3 and MnO_2). However, it pulls irrelevant lithium compounds (Li_2CO_3 and LiOH) into the recipe and overlooks the fact that metathesis reactions (Li et al., 2015; Todd et al., 2021) require less applied energy than high-temperature sintering, which relies on solid-state diffusion (Maximenko & Olevsky, 2004). Vanilla LLMs also exhibit uncertainty about specific synthesis details, such as heating temperature, duration, cooling rate, *etc*. In some edge cases such as $LiFePO_4$ presented in Table B6.10, the cited references are associated with the real papers but the contents are dissociated from the cited titel and hallucinated from the pre-training corpus.

We further compare the performance of LLaMP on synthesizability prediction with stoichiometric convolutional graph neural fingerprint (stoi-CGNF) (Jang et al., 2024) and fine-tuned LLMs (Kim et al., 2024). We follow the positive-unlabeled (PU) classification task proposed in (Kim et al., 2024) by randomly selecting a subset of positive (probable) and unlabeled (unlikely) inorganic compounds and compare the classification performances of LLaMP with different backend LLMs and baselines. As presented in Table 3, LLaMP effectively enhances the performances of backbone GPT-4 and

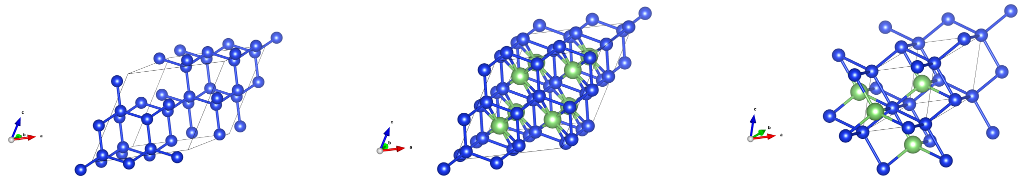

(a) MP ground truth (DC Si, mp-149)

(b) LLaMP (DC Si with Li hexagonal interstitial)

(c) GPT-3.5 (distorted Si with Li tetrahedral interstitial)

Figure 3: Generation and manipulation of crystal structures using LLMs to insert an additional lithium atom at the interstitial site in diamond cubic silicon structure. Blue: Si. Green: Li. Question-answer pairs are listed in Table B6.11. Additional atoms extended through bonds are visualized.

Table 4: Structural parameters of the generated crystals compared with diamond cubic (DC) silicon. From left to right are fractional coordinates of inserted Li atom $(x, y, z)_{\text{Li}}$, total cell volume V, average Si−Si bond lengths ℓ_{SiSi}, Si−Si−Si angles θ_{SiSiSi}, and Si−Li−Si angles θ_{SiLiSi}. GPT-4 refuses to respond due to their safeguard against the lack of atomic structure information.

	$(x, y, z)_{\text{Li}}$	ℓ_{SiSi} (Å)	Error (%)	V (Å^3)	Error (%)	θ_{SiSiSi} (°)	Error (%)	θ_{SiLiSi} (°)
LLaMP	$(0.5, 0.5, 0.5)$	2.36	**0.0**	40.33	**0.0**	109.47	**0.0**	62.96
GPT-3.5	$(0.5, 0.5, 0.5)$	2.71	+15.0	67.05	+66.3	98.28	-10.2	67.69
GPT-4	-	-	-	-	-	-	-	-
DC Si (mp-149)		2.36		40.33		109.47		

Sonnet LLMs by a significant margin of 20%, with the classification precision of LLaMP (GPT-4) up to 0.895.

Table 3: Positive-unlabeled (PU) classification of LLaMP and baseline methods on inorganic material synthesizablity. (*) Evaluations on 352,236 positive and 40,817 unlabeled compounds by Kim et al. (2024).

	Accuracy	F1	Precision	Recall
LLaMP (GPT-4)	0.800	0.773	**0.895**	0.680
LLaMP (Sonnet)	**0.818**	**0.812**	0.848	0.780
GPT-4	0.600	0.649	0.578	0.740
Sonnet	0.530	0.230	0.636	0.140
Llama3	0.480	0.623	0.489	**0.860**
Gemini	0.590	0.388	0.765	0.260
GPT-4*	-	-	0.151	0.620
GPT-3.5 (FT)*	-	-	**0.558**	**0.951**
stoi-CGNF*	-	-	0.541	0.942

RAG-assisted crystal editing Fine-tuned LLMs for text-encoded atomistic information have shown the capability to generate stable crystals under the constraints of atomic positions and charges (Gruver et al., 2023). In this context, we delve into the examination and comparison of the crystal editing capabilities between LLaMP and GPT-3.5, without resorting to fine-tuning or tailored prompt messages in previous work. Figure 3 showcases the structures generated by LLaMP and vanilla GPT-3.5 without RAG, both instructed to *insert one lithium atom at the tetrahedral site of the diamond cubic silicon structure* (Table B6.11). Notably, both LLaMP and GPT-3.5 place an additional Li atom at fractional coordinate $(0.5, 0.5, 0.5)$. However, the Si structure retrieved by LLaMP adheres to the MP convention, positioning two Si bases at $(0.125, 0.125, 0.125)$ and $(0.875, 0.875, 0.875)$. This causes the inserted Li atom to be *hexagonal interstitial* instead of *tetrahedral interstitial*.

GPT-3.5 locates the Li atom at the tetrahedral site given the "luckily chosen" Si bases at $(0, 0, 0)$ and $(0.25, 0.25, 0.25)$; however, the resulting cell volume and shape are highly distorted, and the Si−Si bond length and Si−Si−Si angle deviate significantly from the ground truth (Table 4), highlighting the limitations in the intrinsic encoding of LLMs for atomistic information and the challenges associated with zero-shot generation of crystal structures. In contrast, the LLaMP-retrieved MP structure serves as a robust prior, anchoring the lattice parameters of the generated structure to the correct values.

Language-driven simulation LLaMP equipped with Python REPL and atomistic simulation workflow package `atomate2` performs well out of the box for complex multi-step simulations using pre-trained universal interatomic potential MACE-MP-0 (Batatia et al., 2023) through language instruction. As demonstrated in Appendix C, LLaMP is able to follow multi-step instructions to fetch stable crystal structure from MP, generate a supercell of atomic structure, and run annealing molecular dynamics simulation with varying temperatures from 300K to 800K and back to 300K. After the simulation is finished, LLaMP can read the simulation trajectories and plot the temperature profile over time (Appendix C.1).

We further test the robustness of our language-driven workflow by randomly selecting 50 supercell up-to-quinary structure compounds in MP. Each MD simulation runs $0.1\,\mathrm{ps}$ with timestep of $2\,\mathrm{fs}$. The timeout was set to 90 seconds. 96% workflows were successfully initiated, with 62% finished and 34% of systems exceeding 90 seconds timeout due to slow or stalled MACE-MP-0 runs (the simulation is still running without error but runs slowly). 4% simulations ran into unspecified status. We found that during these triggered workflows, LLaMP asks the user for approval on the precise chemical formula to fetch the structure from MP, rendering the workflow unfinished.

4.3 Analysis

Multimodal material property retrieval Materials design often involves multi-objective property optimization. These properties span a Pareto front where optimizing one factor incurs deterioration in others. To succeed in such tasks, combining different modalities of materials properties is necessary. LLaMP achieves this through the hierarchical orchestration. For the example question "*What's the stiffest material with the lowest formation energy in Si-O system?*" (Figure A.1), when a query requires multimodal information and compound logic, the supervisor agent decomposes the query into multiple subtasks, delegates them to assistant agents (`MPThermoExpert` and `MPElasticityExpert`) for information retrieval, and in the final stage of reasoning integrates information from both modalities, drawing on the context in episodic memory retrieved from the assistant agents (Figure 1). This enables LLaMP to perform various tasks step-by-step by combining multiple data sources from the Materials Project (MP) (*e.g.* 3D crystal structures, thermodynamic, mechanical, magnetic properties, and more listed in Appendix A.2) in a single query.

Failure and safeguard modes In scientific research, refusing ambiguous or unsupported queries is critical to ensuring reliability. LLaMP demonstrates this capability by identifying limitations in data availability or query specificity and providing appropriate responses. For instance, when asked for the bulk modulus of "stainless steel," LLaMP points out the ambiguity of the query due to variable compositions. Similarly, it flags unavailable synthesis recipes or computed properties for specific materials. Examples of these safeguard modes can be found in Appendix A.5.

5 Conclusion

We introduce LLaMP, a hierarchical multi-agent framework that integrates LLMs with high-fidelity material informatics and domain-specific workflows for scientific research. By leveraging modular agents and robust hierarchical planning, LLaMP bridges the gap between general-purpose LLMs and complex materials science experimental workflows. Our results demonstrate that LLaMP consistently outperforms baseline methods across diverse tasks, including material property prediction, crystal structure manipulation, and multimodal data retrieval. Through grounding in expert-verified databases and iterative self-correction, LLaMP mitigates hallucination, enhances response consistency, and enables complex experimental simulations.

Limitation LLaMP's effectiveness relies on the backbone LLM's function-calling and reasoning capabilities, which can sometimes misinterpret schema descriptions, leading to unexpected behaviors. Its accuracy is further influenced by the quality of theoretical predictions and the comprehensiveness of the Materials Project (MP) database. For example, underpredicted bandgaps by GGA functional and the incomplete search for magnetic configurations—focusing primarily on high-spin ferromagnetic states—may overlook antiferromagnetic ground states below the energy convex hull. While MP is among the most comprehensive materials databases, it is not exhaustive and would benefit from incorporating additional intermetallic compounds and high-entropy materials from databases like AFLOW, OQMD, and NOMAD (Merchant et al., 2023; Curtarolo et al., 2012b; Kirklin et al., 2015b; Scheidgen et al., 2023a).

References

Bang, Y., Cahyawijaya, S., Lee, N., Dai, W., Su, D., Wilie, B., Lovenia, H., Ji, Z., Yu, T., Chung, W., Do, Q. V., Xu, Y., and Fung, P. A Multitask, Multilingual, Multimodal Evaluation of ChatGPT on Reasoning, Hallucination, and Interactivity, November 2023. URL http://arxiv.org/abs/2302.04023. arXiv:2302.04023 [cs].

Batatia, I., Benner, P., Chiang, Y., Elena, A. M., Kovács, D. P., Riebesell, J., Advincula, X. R., Asta, M., Baldwin, W. J., Bernstein, N., Bhowmik, A., Blau, S. M., Cărare, V., Darby, J. P., De, S., Della Pia, F., Deringer, V. L., Elijošius, R., El-Machachi, Z., Fako, E., Ferrari, A. C., Genreith-Schriever, A., George, J., Goodall, R. E. A., Grey, C. P., Han, S., Handley, W., Heenen, H. H., Hermansson, K., Holm, C., Jaafar, J., Hofmann, S., Jakob, K. S., Jung, H., Kapil, V., Kaplan, A. D., Karimitari, N., Kroupa, N., Kullgren, J., Kuner, M. C., Kuryla, D., Liepuoniute, G., Margraf, J. T., Magdău, I.-B., Michaelides, A., Moore, J. H., Naik, A. A., Niblett, S. P., Norwood, S. W., O'Neill, N., Ortner, C., Persson, K. A., Reuter, K., Rosen, A. S., Schaaf, L. L., Schran, C., Sivonxay, E., Stenczel, T. K., Svahn, V., Sutton, C., van der Oord, C., Varga-Umbrich, E., Vegge, T., Vondrák, M., Wang, Y., Witt, W. C., Zills, F., and Csányi, G. A foundation model for atomistic materials chemistry, December 2023. URL http://arxiv.org/abs/2401.00096. arXiv:2401.00096 [cond-mat, physics:physics].

Boiko, D. A., MacKnight, R., Kline, B., and Gomes, G. Autonomous chemical research with large language models. *Nature*, 624(7992):570–578, December 2023. ISSN 1476-4687. doi: 10.1038/s41586-023-06792-0. URL https://www.nature.com/articles/s41586-023-06792-0. Number: 7992 Publisher: Nature Publishing Group.

Borlido, P., Schmidt, J., Huran, A. W., Tran, F., Marques, M. A. L., and Botti, S. Exchange-correlation functionals for band gaps of solids: benchmark, reparametrization and machine learning. *npj Computational Materials*, 6(1):1–17, July 2020. ISSN 2057-3960. doi: 10.1038/s41524-020-00360-0. URL https://www.nature.com/articles/s41524-020-00360-0. Number: 1 Publisher: Nature Publishing Group.

Cha, J., Kang, W., Mun, J., and Roh, B. Honeybee: Locality-enhanced Projector for Multimodal LLM, April 2024. URL http://arxiv.org/abs/2312.06742. arXiv:2312.06742.

Chase, H. LangChain, October 2022. URL https://github.com/langchain-ai/langchain.

Curtarolo, S., Setyawan, W., Hart, G. L., Jahnatek, M., Chepulskii, R. V., Taylor, R. H., Wang, S., Xue, J., Yang, K., Levy, O., et al. Aflow: An automatic framework for high-throughput materials discovery. *Computational Materials Science*, 58:218–226, 2012a.

Curtarolo, S., Setyawan, W., Hart, G. L. W., Jahnatek, M., Chepulskii, R. V., Taylor, R. H., Wang, S., Xue, J., Yang, K., Levy, O., Mehl, M. J., Stokes, H. T., Demchenko, D. O., and Morgan, D. AFLOW: An automatic framework for high-throughput materials discovery. *Computational Materials Science*, 58:218–226, June 2012b. ISSN 0927-0256. doi: 10.1016/j.commatsci.2012.02.005. URL https://www.sciencedirect.com/science/article/pii/S0927025612000717.

Dagdelen, J., Dunn, A., Lee, S., Walker, N., Rosen, A. S., Ceder, G., Persson, K. A., and Jain, A. Structured information extraction from scientific text with large language models. *Nature Communications*, 15(1):1418, February 2024. ISSN 2041-1723. doi: 10.1038/s41467-024-45563-x. URL https://www.nature.com/articles/s41467-024-45563-x. Publisher: Nature Publishing Group.

Du, Y., Wei, F., and Zhang, H. Anytool: Self-reflective, hierarchical agents for large-scale api calls. *arXiv preprint arXiv:2402.04253*, 2024.

Frey, N., Soklaski, R., Axelrod, S., Samsi, S., Gomez-Bombarelli, R., Coley, C., and Gadepally, V. Neural Scaling of Deep Chemical Models, May 2022. URL https://chemrxiv.org/engage/chemrxiv/article-details/627bddd544bdd532395fb4b5.

Ghafarollahi, A. and Buehler, M. J. AtomAgents: Alloy design and discovery through physics-aware multi-modal multi-agent artificial intelligence, July 2024. URL http://arxiv.org/abs/2407.10022. arXiv:2407.10022.

Gruver, N., Sriram, A., Madotto, A., Wilson, A., Zitnick, C. L., and Ulissi, Z. Fine-Tuned Language Models Generate Stable Inorganic Materials as Text. November 2023. URL https://openreview.net/forum?id=0r5DE2ZSwJ.

Gupta, T., Zaki, M., Krishnan, N. M. A., and Mausam. MatSciBERT: A materials domain language model for text mining and information extraction. *npj Computational Materials*, 8(1):1–11, May 2022. ISSN 2057-3960. doi: 10.1038/s41524-022-00784-w. URL https://www.nature.com/articles/s41524-022-00784-w. Number: 1 Publisher: Nature Publishing Group.

Hira, K., Zaki, M., Sheth, D., Mausam, and Krishnan, N. M. A. Reconstructing the materials tetrahedron: challenges in materials information extraction. *Digital Discovery*, 3(5):1021–1037, 2024. ISSN 2635-098X. doi: 10.1039/D4DD00032C. URL https://xlink.rsc.org/?DOI=D4DD00032C.

Jablonka, K. M., Schwaller, P., Ortega-Guerrero, A., and Smit, B. Leveraging large language models for predictive chemistry. *Nature Machine Intelligence*, 6(2):161–169, February 2024. ISSN 2522-5839. doi: 10.1038/s42256-023-00788-1. URL https://www.nature.com/articles/s42256-023-00788-1. Publisher: Nature Publishing Group.

Jain, A., Ong, S. P., Hautier, G., Chen, W., Richards, W. D., Dacek, S., Cholia, S., Gunter, D., Skinner, D., Ceder, G., and Persson, K. A. Commentary: The Materials Project: A materials genome approach to accelerating materials innovation. *APL Materials*, 1(1):011002, July 2013. ISSN 2166-532X. doi: 10.1063/1.4812323. URL https://doi.org/10.1063/1.4812323.

Jang, J., Noh, J., Zhou, L., Gu, G. H., Gregoire, J. M., and Jung, Y. Synthesizability of materials stoichiometry using semi-supervised learning. *Matter*, 7(6):2294–2312, June 2024. ISSN 2590-2393, 2590-2385. doi: 10.1016/j.matt.2024.05.002. URL https://www.cell.com/matter/abstract/S2590-2385(24)00227-3. Publisher: Elsevier.

Kim, S., Jung, Y., and Schrier, J. Large Language Models for Inorganic Synthesis Predictions. *Journal of the American Chemical Society*, 146(29):19654–19659, July 2024. ISSN 0002-7863. doi: 10.1021/jacs.4c05840. URL https://doi.org/10.1021/jacs.4c05840. Publisher: American Chemical Society.

Kirklin, S., Saal, J., Meredig, B., Thompson, A., Doak, J., Aykol, M., Rühl, S., and Wolverton, C. The open quantum materials database (oqmd): Assessing the accuracy of dft formation energies. *npj Computational Materials*, 1:15010, 12 2015a. doi: 10.1038/npjcompumats.2015.10.

Kirklin, S., Saal, J. E., Meredig, B., Thompson, A., Doak, J. W., Aykol, M., Rühl, S., and Wolverton, C. The Open Quantum Materials Database (OQMD): assessing the accuracy of DFT formation energies. *npj Computational Materials*, 1(1):1–15, December 2015b. ISSN 2057-3960. doi: 10.1038/npjcompumats.2015.10. URL https://www.nature.com/articles/npjcompumats201510. Publisher: Nature Publishing Group.

Kononova, O., Huo, H., He, T., Rong, Z., Botari, T., Sun, W., Tshitoyan, V., and Ceder, G. Text-mined dataset of inorganic materials synthesis recipes. *Scientific Data*, 6(1):203, October 2019. ISSN 2052-4463. doi: 10.1038/s41597-019-0224-1. URL https://www.nature.com/articles/s41597-019-0224-1. Number: 1 Publisher: Nature Publishing Group.

Kresse, G. and Furthmüller, J. Efficient iterative schemes for ab initio total-energy calculations using a plane-wave basis set. *Physical Review B*, 54(16):11169–11186, October 1996. doi: 10.1103/PhysRevB.54.11169. URL https://link.aps.org/doi/10.1103/PhysRevB.54.11169. Publisher: American Physical Society.

Lewis, P., Perez, E., Piktus, A., Petroni, F., Karpukhin, V., Goyal, N., Küttler, H., Lewis, M., Yih, W.-t., Rocktäschel, T., Riedel, S., and Kiela, D. Retrieval-Augmented Generation for Knowledge-Intensive NLP Tasks. In *Advances in Neural Information Processing Systems*, volume 33, pp. 9459–9474. Curran Associates, Inc., 2020. URL https://proceedings.neurips.cc/paper/2020/hash/6b493230205f780e1bc26945df7481e5-Abstract.html.

Lewis, P., Perez, E., Piktus, A., Petroni, F., Karpukhin, V., Goyal, N., Küttler, H., Lewis, M., Yih, W.-t., Rocktäschel, T., Riedel, S., and Kiela, D. Retrieval-Augmented Generation for Knowledge-Intensive NLP Tasks, April 2021. URL http://arxiv.org/abs/2005.11401. arXiv:2005.11401 [cs] version: 4.

Li, J., Smith, A. E., Jiang, P., Stalick, J. K., Sleight, A. W., and Subramanian, M. A. True Composition and Structure of Hexagonal "YAlO3", Actually Y3Al3O8CO3. *Inorganic Chemistry*, 54(3):837–844, February 2015. ISSN 0020-1669. doi: 10.1021/ic502027k. URL https://doi.org/10.1021/ic502027k. Publisher: American Chemical Society.

Liang, P., Bommasani, R., Lee, T., Tsipras, D., Soylu, D., Yasunaga, M., Zhang, Y., Narayanan, D., Wu, Y., Kumar, A., Newman, B., Yuan, B., Yan, B., Zhang, C., Cosgrove, C., Manning, C. D., Ré, C., Acosta-Navas, D., Hudson, D. A., Zelikman, E., Durmus, E., Ladhak, F., Rong, F., Ren, H., Yao, H., Wang, J., Santhanam, K., Orr, L., Zheng, L., Yuksekgonul, M., Suzgun, M., Kim, N., Guha, N., Chatterji, N., Khattab, O., Henderson, P., Huang, Q., Chi, R., Xie, S. M., Santurkar, S., Ganguli, S., Hashimoto, T., Icard, T., Zhang, T., Chaudhary, V., Wang, W., Li, X., Mai, Y., Zhang, Y., and Koreeda, Y. Holistic Evaluation of Language Models, October 2023. URL http://arxiv.org/abs/2211.09110. arXiv:2211.09110 [cs].

Lu, C., Lu, C., Lange, R. T., Foerster, J., Clune, J., and Ha, D. The ai scientist: Towards fully automated open-ended scientific discovery. *arXiv preprint arXiv:2408.06292*, 2024.

Luo, Y., Liu, C., and Ji, S. Towards Symmetry-Aware Generation of Periodic Materials, July 2023. URL https://arxiv.org/abs/2307.02707v2.

M. Bran, A., Cox, S., Schilter, O., Baldassari, C., White, A. D., and Schwaller, P. Augmenting large language models with chemistry tools. *Nature Machine Intelligence*, pp. 1–11, May 2024. ISSN 2522-5839. doi: 10.1038/s42256-024-00832-8. URL https://www.nature.com/articles/s42256-024-00832-8. Publisher: Nature Publishing Group.

Mallen, A., Asai, A., Zhong, V., Das, R., Khashabi, D., and Hajishirzi, H. When Not to Trust Language Models: Investigating Effectiveness of Parametric and Non-Parametric Memories, July 2023. URL http://arxiv.org/abs/2212.10511. arXiv:2212.10511 [cs].

Maximenko, A. L. and Olevsky, E. A. Effective diffusion coefficients in solid-state sintering. *Acta Materialia*, 52(10):2953–2963, June 2004. ISSN 1359-6454. doi: 10.1016/j.actamat.2004.02.042. URL https://www.sciencedirect.com/science/article/pii/S1359645404001326.

Merchant, A., Batzner, S., Schoenholz, S. S., Aykol, M., Cheon, G., and Cubuk, E. D. Scaling deep learning for materials discovery. *Nature*, pp. 1–6, November 2023. ISSN 1476-4687. doi: 10.1038/s41586-023-06735-9. URL https://www.nature.com/articles/s41586-023-06735-9. Publisher: Nature Publishing Group.

Miret, S. and Krishnan, N. M. A. Are LLMs Ready for Real-World Materials Discovery?, September 2024. URL http://arxiv.org/abs/2402.05200. arXiv:2402.05200 [cond-mat].

Ouyang, S., Zhang, Z., Yan, B., Liu, X., Choi, Y., Han, J., and Qin, L. Structured Chemistry Reasoning with Large Language Models, February 2024. URL http://arxiv.org/abs/2311.09656. arXiv:2311.09656 [cs].

Pilania, G., Gubernatis, J. E., and Lookman, T. Multi-fidelity machine learning models for accurate bandgap predictions of solids. *Computational Materials Science*, 129:156–163, March 2017. ISSN 0927-0256. doi: 10.1016/j.commatsci.2016.12.004. URL https://www.sciencedirect.com/science/article/pii/S0927025616306188.

Polak, M. P. and Morgan, D. Extracting Accurate Materials Data from Research Papers with Conversational Language Models and Prompt Engineering, June 2023. URL http://arxiv.org/abs/2303.05352. arXiv:2303.05352 [cond-mat].

Qin, Y., Liang, S., Ye, Y., Zhu, K., Yan, L., Lu, Y., Lin, Y., Cong, X., Tang, X., Qian, B., Zhao, S., Hong, L., Tian, R., Xie, R., Zhou, J., Gerstein, M., Li, D., Liu, Z., and Sun, M. ToolLLM: Facilitating Large Language Models to Master 16000+ Real-world APIs, October 2023. URL http://arxiv.org/abs/2307.16789. arXiv:2307.16789.

Rubungo, A. N., Li, K., Hattrick-Simpers, J., and Dieng, A. B. Llm4mat-bench: Benchmarking large language models for materials property prediction. *arXiv preprint arXiv:2411.00177*, 2024.

Scheidgen, M., Himanen, L., Ladines, A. N., Sikter, D., Nakhaee, M., Fekete, , Chang, T., Golparvar, A., Márquez, J. A., Brockhauser, S., Brückner, S., Ghiringhelli, L. M., Dietrich, F., Lehmberg, D., Denell, T., Albino, A., Näsström, H., Shabih, S., Dobener, F., Kühbach, M., Mozumder, R., Rudzinski, J. F., Daelman, N., Pizarro, J. M., Kuban, M., Salazar, C., Ondračka, P., Bungartz, H.-J., and Draxl, C. NOMAD: A distributed web-based platform for managing materials science research data. *Journal of Open Source Software*, 8(90):5388, October 2023a. ISSN 2475-9066. doi: 10.21105/joss.05388. URL https://joss.theoj.org/papers/10.21105/joss.05388.

Scheidgen, M., Himanen, L., Ladines, A. N., Sikter, D., Nakhaee, M., Ádám Fekete, Chang, T., Golparvar, A., Márquez, J. A., Brockhauser, S., Brückner, S., Ghiringhelli, L. M., Dietrich, F., Lehmberg, D., Denell, T., Albino, A., Näsström, H., Shabih, S., Dobener, F., Kühbach, M., Mozumder, R., Rudzinski, J. F., Daelman, N., Pizarro, J. M., Kuban, M., Salazar, C., Ondračka, P., Bungartz, H.-J., and Draxl, C. Nomad: A distributed web-based platform for managing materials science research data. *Journal of Open Source Software*, 8(90):5388, 2023b. doi: 10.21105/joss.05388. URL https://doi.org/10.21105/joss.05388.

Schilling-Wilhelmi, M., Ríos-García, M., Shabih, S., Gil, M. V., Miret, S., Koch, C. T., Márquez, J. A., and Jablonka, K. M. From Text to Insight: Large Language Models for Materials Science Data Extraction, July 2024. URL http://arxiv.org/abs/2407.16867. arXiv:2407.16867.

Shao, Y., Gan, Z., Epifanovsky, E., Gilbert, A. T., Wormit, M., Kussmann, J., Lange, A. W., Behn, A., Deng, J., Feng, X., Ghosh, D., Goldey, M., Horn, P. R., Jacobson, L. D., Kaliman, I., Khaliullin, R. Z., Kuś, T., Landau, A., Liu, J., Proynov, E. I., Rhee, Y. M., Richard, R. M., Rohrdanz, M. A., Steele, R. P., Sundstrom, E. J., Woodcock III, H. L., Zimmerman, P. M., Zuev, D., Albrecht, B., Alguire, E., Austin, B., Beran, G. J. O., Bernard, Y. A., Berquist, E., Brandhorst, K., Bravaya, K. B., Brown, S. T., Casanova, D., Chang, C.-M., Chen, Y., Chien, S. H., Closser, K. D., Crittenden, D. L., Diedenhofen, M., DiStasio Jr., R. A., Do, H., Dutoi, A. D., Edgar, R. G., Fatehi, S., Fusti-Molnar, L., Ghysels, A., Golubeva-Zadorozhnaya, A., Gomes, J., Hanson-Heine, M. W., Harbach, P. H., Hauser, A. W., Hohenstein, E. G., Holden, Z. C., Jagau, T.-C., Ji, H., Kaduk, B., Khistyaev, K., Kim, J., Kim, J., King, R. A., Klunzinger, P., Kosenkov, D., Kowalczyk, T., Krauter, C. M., Lao, K. U., Laurent, A. D., Lawler, K. V., Levchenko, S. V., Lin, C. Y., Liu, F., Livshits, E., Lochan, R. C., Luenser, A., Manohar, P., Manzer, S. F., Mao, S.-P., Mardirossian, N., Marenich, A. V., Maurer, S. A., Mayhall, N. J., Neuscamman, E., Oana, C. M., Olivares-Amaya, R., O'Neill, D. P., Parkhill, J. A., Perrine, T. M., Peverati, R., Prociuk, A., Rehn, D. R., Rosta, E., Russ, N. J., Sharada, S. M., Sharma, S., Small, D. W., Sodt, A., Stein, T., Stück, D., Su, Y.-C., Thom, A. J., Tsuchimochi, T., Vanovschi, V., Vogt, L., Vydrov, O., Wang, T., Watson, M. A., Wenzel, J., White, A., Williams, C. F., Yang, J., Yeganeh, S., Yost, S. R., You, Z.-Q., Zhang, I. Y., Zhang, X., Zhao, Y., Brooks, B. R., Chan, G. K., Chipman, D. M., Cramer, C. J., Goddard III, W. A., Gordon, M. S., Hehre, W. J., Klamt, A., Schaefer III, H. F., Schmidt, M. W., Sherrill, C. D., Truhlar, D. G., Warshel, A., Xu, X., Aspuru-Guzik, A., Baer, R., Bell, A. T., Besley, N. A., Chai, J.-D., Dreuw, A., Dunietz, B. D., Furlani, T. R., Gwaltney, S. R., Hsu, C.-P., Jung, Y., Kong, J., Lambrecht, D. S., Liang, W., Ochsenfeld, C., Rassolov, V. A., Slipchenko, L. V., Subotnik, J. E., Van Voorhis, T., Herbert, J. M., Krylov, A. I., Gill, P. M., and Head-Gordon, M. Advances in molecular quantum chemistry contained in the Q-Chem 4 program package. *Molecular Physics*, 113(2): 184–215, January 2015. ISSN 0026-8976. doi: 10.1080/00268976.2014.952696. URL https://www.tandfonline.com/doi/full/10.1080/00268976.2014.952696. Publisher: Taylor & Francis.

Shinn, N., Cassano, F., Berman, E., Gopinath, A., Narasimhan, K., and Yao, S. Reflexion: Language Agents with Verbal Reinforcement Learning, October 2023. URL http://arxiv.org/abs/2303.11366. arXiv:2303.11366 [cs].

Song, Y., Miret, S., and Liu, B. MatSci-NLP: Evaluating Scientific Language Models on Materials Science Language Tasks Using Text-to-Schema Modeling, May 2023. URL http://arxiv.org/abs/2305.08264. arXiv:2305.08264.

Spotte-Smith, E. W. C., Cohen, O. A., Blau, S., Munro, J., Yang, R., Guha, R., Patel, H., Vijay, S., Huck, P., Kingsbury, R., Horton, M., and Persson, K. A database of molecular properties integrated in the Materials Project, October 2023. URL https://chemrxiv.org/engage/chemrxiv/article-details/651a3302ade1178b247ee6d1.

Todd, P. K., McDermott, M. J., Rom, C. L., Corrao, A. A., Denney, J. J., Dwaraknath, S. S., Khalifah, P. G., Persson, K. A., and Neilson, J. R. Selectivity in Yttrium Manganese Oxide Synthesis via Local Chemical Potentials in Hyperdimensional Phase Space. *Journal of the American Chemical Society*, 143(37):15185–15194, September 2021. ISSN 0002-7863. doi: 10.1021/jacs.1c06229. URL https://doi.org/10.1021/jacs.1c06229. Publisher: American Chemical Society.

Wang, L., Ma, C., Feng, X., Zhang, Z., Yang, H., Zhang, J., Chen, Z., Tang, J., Chen, X., Lin, Y., et al. A survey on large language model based autonomous agents. *Frontiers of Computer Science*, 18(6):186345, 2024.

Wang, X., Hu, Z., Lu, P., Zhu, Y., Zhang, J., Subramaniam, S., Loomba, A. R., Zhang, S., Sun, Y., and Wang, W. Scibench: Evaluating college-level scientific problem-solving abilities of large language models. *arXiv preprint arXiv:2307.10635*, 2023.

Wen, M., Spotte-Smith, E. W. C., Blau, S. M., McDermott, M. J., Krishnapriyan, A. S., and Persson, K. A. Chemical reaction networks and opportunities for machine learning. *Nature Computational Science*, 3(1):12–24, January 2023. ISSN 2662-8457. doi: 10.1038/s43588-022-00369-z. URL https://www.nature.com/articles/s43588-022-00369-z. Publisher: Nature Publishing Group.

Wen, M., Horton, M. K., Munro, J. M., Huck, P., and Persson, K. A. An equivariant graph neural network for the elasticity tensors of all seven crystal systems. *Digital Discovery*, 3(5):869–882, May 2024. ISSN 2635-098X. doi: 10.1039/D3DD00233K. URL https://pubs.rsc.org/en/content/articlelanding/2024/dd/d3dd00233k. Publisher: RSC.

Xie, T., Wan, Y., Huang, W., Yin, Z., Liu, Y., Wang, S., Linghu, Q., Kit, C., Grazian, C., Zhang, W., Razzak, I., and Hoex, B. DARWIN Series: Domain Specific Large Language Models for Natural Science, August 2023. URL http://arxiv.org/abs/2308.13565. arXiv:2308.13565 [cond-mat, physics:physics].

Xu, Z., Jain, S., and Kankanhalli, M. Hallucination is Inevitable: An Innate Limitation of Large Language Models, January 2024. URL http://arxiv.org/abs/2401.11817. arXiv:2401.11817 [cs].

Yan, F., Mao, H., Ji, C. C.-J., Zhang, T., Patil, S. G., Stoica, I., and Gonzalez, J. E. Berkeley Function Calling Leaderboard. 2024. URL https://gorilla.cs.berkeley.edu/blogs/8_berkeley_function_calling_leaderboard.html.

Yang, S., Li, S., Venugopalan, S., Tshitoyan, V., Aykol, M., Merchant, A., Cubuk, E., and Cheon, G. Accurate Prediction of Experimental Band Gaps from Large Language Model-Based Data Extraction. November 2023. URL https://openreview.net/forum?id=oRKWhmtUG6.

Yao, S., Zhao, J., Yu, D., Du, N., Shafran, I., Narasimhan, K., and Cao, Y. ReAct: Synergizing Reasoning and Acting in Language Models, March 2023. URL http://arxiv.org/abs/2210.03629. arXiv:2210.03629 [cs].

Zagorac, D., Müller, H., Ruehl, S., Zagorac, J., and Rehme, S. Recent developments in the Inorganic Crystal Structure Database: theoretical crystal structure data and related features. *Journal of Applied Crystallography*, 52(5):918–925, October 2019. ISSN 1600-5767. doi: 10.1107/S160057671900997X. URL https://journals.iucr.org/j/issues/2019/05/00/in5024/. Publisher: International Union of Crystallography.

Zaki, M., Jayadeva, Mausam, and Krishnan, N. M. A. MaScQA: A Question Answering Dataset for Investigating Materials Science Knowledge of Large Language Models, August 2023. URL http://arxiv.org/abs/2308.09115. arXiv:2308.09115.

Zeni, C., Pinsler, R., Zügner, D., Fowler, A., Horton, M., Fu, X., Shysheya, S., Crabbé, J., Sun, L., Smith, J., Nguyen, B., Schulz, H., Lewis, S., Huang, C.-W., Lu, Z., Zhou, Y., Yang, H., Hao, H., Li, J., Tomioka, R., and Xie, T. MatterGen: a generative model for inorganic materials design, January 2024. URL http://arxiv.org/abs/2312.03687. arXiv:2312.03687 [cond-mat].

Zhang, H., Song, Y., Hou, Z., Miret, S., and Liu, B. HoneyComb: A Flexible LLM-Based Agent System for Materials Science, August 2024. URL http://arxiv.org/abs/2409.00135. arXiv:2409.00135.

Zheng, Z., Zhang, O., Borgs, C., Chayes, J. T., and Yaghi, O. M. ChatGPT Chemistry Assistant for Text Mining and Prediction of MOF Synthesis. *Journal of the American Chemical Society*, 145(32):18048–18062, August 2023. ISSN 0002-7863, 1520-5126. doi: 10.1021/jacs.3c05819. URL http://arxiv.org/abs/2306.11296. arXiv:2306.11296 [cond-mat, physics:physics].

A SUPPLEMENTARY INFORMATION

A.1 EXAMPLE WORKFLOW

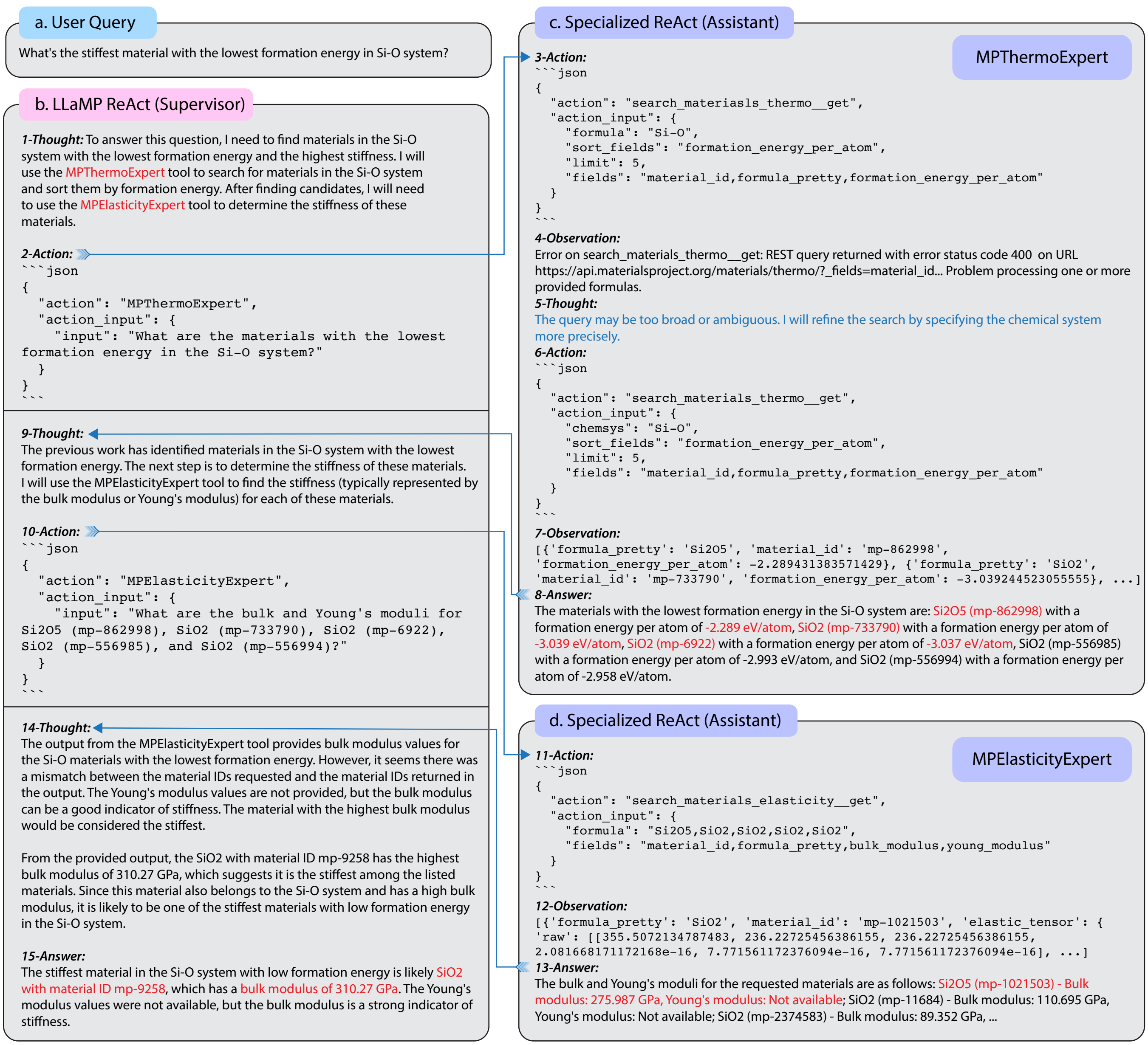

Figure A.1: Multimodal retrieval-augmented generation for materials informatics. (a) User query. (b) Supervisor ReAct agent capable of handling multiple assistant agents and high-level reasoning. (c-d) Assistant ReAct agents executing function calling and summarization. (c) `MPThermoExpert` and (d) `MPElasticityExpert` have access to the API schemas of thermo and elasticity endpoints on Materials Project, respectively. The selected details are highlighted in red, demonstrating the capabilities of RAG and ReAct implemented in LLaMP. The blue texts show LLaMP assistant ReAct agent can handle API calling errors and self-correct the input query accordingly.

A.2 List of Implemented Assistant Agents and Tools

Here we provide the comprehensive list of implemented **assistant agents** and `tools`. Notably, **MP Assistants** are designed with a highly modular architecture, making it straightforward to extend support for additional API endpoints from https://api.materialsproject.org/docs.

- **MPSummaryExpert**: `summary` provides amalgamated data for a material by combining subsets of data from many of the other API endpoints.
- **MPThermoExpert**: `thermo` provides computed thermodynamic data for a material such as formation energy and energy above hull.
- **MPElasticityExpert**: `elasticity` provides bulk, shear, and Young's modulus, poisson ratio, and universal anisotropy index.
- **MPMagnetismExpert**: `magnetism` provides computed magnetic ordering related data.
- **MPDielectricExpert**: `dielectric` provides computed dielectric data from density functional perturbation theory.
- **MPPiezoelectricExpert**: `piezoelectric` provides computed piezoelectric data from density functional perturbation theory.
- **MPElectronicExpert**: `electronic_structure` provides computed electronic structure related data for a material such as band gap and fermi level. Python objects for line-mode band structures, density of states, and fermi surfaces are also available.
- **MPSynthesisExpert**: `synthesis` provides a synthesis recipes for materials extracted from literature using text mining and natural language processing techniques.
- **MPStructureRetriever**: `MaterialsStructureText` fetches and saves `pymatgen` Structure objects to local JSON files.
- **MLFFAgent**: `MLFFMD` runs molecular dynamics simulations using pre-trained machine learning force fields; `MLFFElastic` calculates the elastic constants of a given material using pre-trained machine learning force fields.
- `PythonREPLTool`: Python REPL that LLMs could run the generated script.
- `ArxivQueryRun`: LangChain built-in tool that LLMs can use to send API request to ArXiv.
- `WikipediaQueryRun`: LangChain built-in tool that LLMs can use to send API reqeust to Wikipedia.

A.3 Metric calculation in Table 1 and Figure A.2

The following procedures are adopted to calculate the metrics for material property regression benchmarks presented in Table 1 and Figure A.2:

1. Each method was presented with the same query asking for the property of multiple materials. Here we ask each method for bulk modulus, formation energy, and electronic bandgap of ten materials. For example, "What are the bulk moduli of the following metals: Sc, Ti, V, Cr, Mn, Fe, Co, Ni, Cu, Zn?".
2. Repeat the same query for five times and collect the responses.
3. The numerical values are extracted and formatted into 2D arrays with the aid by LLMs. If the range is provided in the response (*e.g.* Llama 3), the median value was used.

4. Calculate Precision, CoP, Confidence, and SCoR for each method across five trials on all materials. The code is provided and the pseudocode can be written as follows:

Input:`arr` (2D array of five responses for different materials)
$n \leftarrow$ count of valid responses (non-`NaN` values) in each column of `arr`
$\texttt{prec} \leftarrow \frac{\texttt{nanstd(arr,axis=0)}}{\sqrt{n}}$
$\texttt{cop} \leftarrow \text{mean}(\exp(-\texttt{prec}))$
$\texttt{conf} \leftarrow \text{mean}\left(\frac{n}{\texttt{\# of trials } N}\right)$
$\texttt{scor} \leftarrow \begin{cases} 0 & \text{if } \texttt{conf} = 0 \text{ for all columns} \\ \texttt{cop} \times \texttt{conf} & \text{otherwise} \end{cases}$
$\texttt{prec} \leftarrow \text{mean}(\texttt{prec})$
Output:`prec`, `cop`, `conf`, `scor`

A.4 Material Property Prediction Result

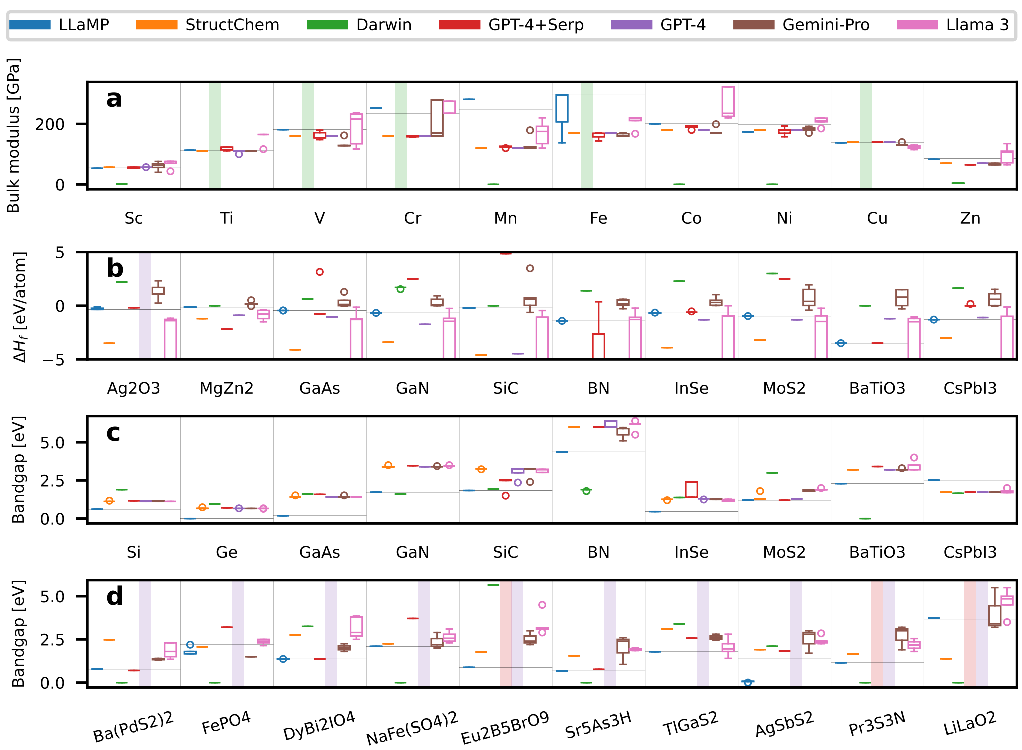

Figure A.2: Boxplot of LLaMP RAG responses, baseline methods, and LLM intrinsic knowledge on material properties. (a) Bulk moduli, K, of 3d transition metals. (b) Formation energies, ΔH_f, of common compounds. (c) Electronic bandgaps, E_g, of common intrinsic semiconductors. (d) Electronic bandgaps of multi-element (ternary or quaternary) materials. Missing predictions are marked by shaded areas. Fliers (Outliers) are marked in circles. Horizontal lines represent the MP reference data. All LLaMP results use GPT-4 as backend language provider. Method with higher SCoR has narrower distribution. LLaMP is effectively grounded on MP reference across different tasks and materials.

A.5 Safeguard or failure modes

- **Question: What is the bulk modulus of stainless steel?** ambiguous chemical formula
  LLaMP: Stainless steel is an alloy with a composition that can vary widely, including elements like iron, chromium, nickel, and molybdenum. Because of this variability, it does

not have a single chemical formula or a unique Materials Project ID, and its bulk modulus can significantly vary based on its exact composition and heat treatment. The Materials Project database, focusing on inorganic crystalline materials, may not provide specific data on complex alloys like stainless steel. For precise values of the bulk modulus, consulting specific datasheets or literature on the type of stainless steel in question is recommended.

- **Question: How to synthesize Y2Be2Fe(SiO5)2?** data unavailable
  LLaMP: Currently, there are no synthesis recipes available in the Materials Project database for Y2Be2Fe(SiO5)2.
- **Question: What's the phonon bandgap of Ac2HgGe?**
  computed property unavailable
  LLaMP: The material Ac2HgGe, with a Materials Project ID of mp-861872, does not have its phonon bandgap information directly available through the Materials Project database. For detailed phonon properties, further analysis using specialized phonon calculation tools or databases would be necessary.

A.6 Compute and time

We compared the runtime of LLaMP against vanilla GPT-4 with 10 runs and computed the average as Table 5 shown. While LLaMP indeed requires more computation time, primarily due to accessing and processing data from the MP database, we emphasize that this additional computational cost is compensated by significantly improved accuracy and self-consistency. Such accuracy improvements are essential in scientific workflows, where precision and reproducibility outweigh the increase in computational overhead.

Table 5: Task Performance Comparison (in seconds)

Task	LLaMP (sec)	GPT-4 (sec)
Bulk Moduli	13.90	4.64
Formation Energy	12.16	2.89
Electronic Bandgap (Common)	25.91	6.33
Electronic Bandgap (Multi-element)	16.15	2.30

A.7 Prompt Template

We use the ReAct template hwchase17/react-multi-input-json from LangChain Hub (https://smith.langchain.com/hub/hwchase17/react-json) as follows:

```
Answer the following questions as best you can. You have access to the following
    tools:

{tools}

The way you use the tools is by specifying a JSON blob.
Specifically, this JSON should have an ‘action‘ key (with the name of the tool to
    use) and an ‘action_input‘ key (with the input to the tool going here).

The only values that should be in the "action" field are: {tool_names}

The $JSON_BLOB should only contain a SINGLE action, do NOT return a list of multiple
     actions. Here is an example of a valid $JSON_BLOB:

‘‘‘
{{
  "action": $TOOL_NAME,
  "action_input": $INPUT
}}
‘‘‘
```

```
ALWAYS use the following format:

Question: the input question you must answer
Thought: you should always think about what to do
Action:
‘‘‘
$JSON_BLOB
‘‘‘
Observation: the result of the action
... (this Thought/Action/Observation can repeat N times)
Thought: I now know the final answer
Final Answer: the final answer to the original input question

Begin! Reminder to always use the exact characters ‘Final Answer‘ when responding.
```

The above system prompt message is prepended with the following solicitation to guide the supervisor agent:

```
You name is LLaMP and you are a helpful agent that can consult materials-related
    data through Materials Project (MP) database, arXiv, Wikipedia, and run
    calculations/simulations via a python REPL and MP atomate2 computational
    workflow.

If you get an error, debug your code and try again. Only use the output of your code
     to answer the question. Ask user to clarify their queries if needed. Please
    note that you don’t have direct control over MP but through multiple assistant
    agents to help you. You need to provide complete context in the input for
    assistants to do their job. REFINE and CRITQUE the output of the assistants if
    needed. You can end the conversation by saying ”Bye”.
```

B SAMPLE QUESTIONS

Table 6: QA comparison between LLaMP and GPT-3.5.

	Question	Answer	
		LLaMP	GPT-3.5
B6.1	What are the bulk moduli of the following metals: Sc, Ti, V, Cr, Mn, Fe, Co, Ni, Cu, Zn?	The bulk moduli of the metals you asked for are as follows (in GPa): - Scandium (Sc): Voigt = 45.715, Reuss = 45.34, VRH = 45.528 - Titanium (Ti): Voigt = 112.955, Reuss = 112.807, VRH = 112.881 - Vanadium (V): Voigt = 181.232, Reuss = 181.232, VRH = 181.232 - Chromium (Cr): Voigt = 252.155, Reuss = 252.155, VRH = 252.155 - Manganese (Mn): Voigt = 280.959, Reuss = 280.959, VRH = 280.959 - Iron (Fe): Voigt = 296.003, Reuss = 295.207, VRH = 295.605 - Cobalt (Co): Voigt = 200.587, Reuss = 200.587, VRH = 200.587 - Nickel (Ni): Voigt = 197.399, Reuss = 197.29, VRH = 197.345 - Copper (Cu): Voigt = 151.394, Reuss = 151.394, VRH = 151.394 - Zinc (Zn): Voigt = 76.283, Reuss = 95.46, VRH = 85.872	The bulk modulus (K) is a measure of a material's resistance to uniform compression. It is defined as the ratio of the change in pressure to the fractional volume compression. The values for the bulk modulus can vary somewhat depending on the specific conditions and crystallographic structures of the materials. The values provided here are approximate and given in gigapascals (GPa): - Scandium (Sc): 55 GPa - Titanium (Ti): 110 GPa - Vanadium (V): 160 GPa - Chromium (Cr): 160 GPa - Manganese (Mn): 120 GPa - Iron (Fe): 170 GPa - Cobalt (Co): 180 GPa - Nickel (Ni): 180 GPa - Copper (Cu): 140 GPa - Zinc (Zn): 70 GPa These values represent typical bulk moduli for these metals, and actual values may vary depending on factors such as temperature and pressure.

Continued on next page

Table 6 – continued from previous page

	Question	**Answer**	
		LLaMP	**GPT-3.5**
B6.2	What is the full elastic tensor of NaCl?	The elastic tensor for NaCl is available for two different entries on Materials Project. For material˙id 'mp-22851', the elastic tensor in IEEE format is [[76.0, 1.0, 1.0, -0.0, 0.0, -0.0], [1.0, 76.0, 1.0, -0.0, -0.0, 0.0], [1.0, 1.0, 76.0, 0.0, -0.0, -0.0], [-0.0, -0.0, 0.0, -3.0, -0.0, -0.0], [0.0, -0.0, -0.0, -0.0, -3.0, 0.0], [-0.0, 0.0, -0.0, -0.0, 0.0, -3.0]]. For material˙id 'mp-22862', the elastic tensor in IEEE format is [[47.0, 12.0, 12.0, 0.0, -0.0, -0.0], [12.0, 47.0, 12.0, 0.0, -0.0, -0.0], [12.0, 12.0, 47.0, 0.0, 0.0, -0.0], [0.0, 0.0, 0.0, 12.0, -0.0, -0.0], [-0.0, -0.0, 0.0, -0.0, 12.0, 0.0], [-0.0, -0.0, -0.0, -0.0, 0.0, 12.0]]	The elastic tensor describes the relationship between stress and strain in a material. It is a 4th-rank tensor that characterizes the elastic properties of a crystal. In the case of NaCl (sodium chloride), the elastic tensor is typically represented by a 6x6 matrix. The elastic constants of NaCl can vary slightly depending on the specific conditions and crystallographic orientation. Here is an approximate form of the elastic tensor for NaCl: C11 = 289.2 GPa C12 = 97.8 GPa C44 = 81.6 GPa C13 = C14 = C15 = C16 = C23 = C24 = C25 = C26 = 0 GPa Note: The values are given in gigapascals (GPa). The elastic constants Cij represent the components of the elastic tensor. In this case, C11, C12, and C44 are the non-zero elastic constants. The off-diagonal terms C13, C14, C15, C16, C23, C24, C25, and C26 are typically zero due to cubic symmetry. Keep in mind that these values are approximate, and there may be slight variations depending on the source and the specific conditions under which the measurements were made. Experimental techniques, such as Brillouin scattering or ultrasonic measurements, are often used to determine the elastic constants of materials.
B6.3	What are the bandgaps of the following materials: Si, Ge, and GaAs, GaN, SiC, BN, InSe, MoS2, BaTiO3, CsPbI3? Only look for ground-state bandgaps.	The ground state bandgaps for the requested materials are as follows: Si: 1.12 eV, Ge: 0.66 eV, GaAs: 1.42 eV, GaN: 3.28 eV, SiC: 2.36 eV, BN: 6.4 eV, InSe: 1.26 eV, MoS2: 1.29 eV, BaTiO3: 3.2 eV, CsPbI3: 1.73 eV. Please note that these values are typical for bulk materials and can vary depending on the specific structure and calculation method.	As of my last knowledge update in January 2022, I can provide you with approximate values for the ground state bandgaps of the materials you mentioned. Keep in mind that these values can vary depending on factors like temperature and crystal structure. Additionally, more recent research may have refined these values. Here are the approximate ground state bandgaps in electron volts (eV): Silicon (Si): 1.1 eV Germanium (Ge): 0.67 eV Gallium Arsenide (GaAs): 1.42 eV Gallium Nitride (GaN): 3.4 eV Silicon Carbide (SiC): 3.2 eV (for 4H-SiC) Boron Nitride (BN): 6 eV Indium Selenide (InSe): 1.25 eV Molybdenum Disulfide (MoS2): 1.3 eV (indirect bandgap) Barium Titanate (BaTiO3): 3.2 eV Cesium Lead Iodide (CsPbI3): 1.7 eV Please note that these values are general approximations and may not represent the specific conditions or variations in different forms of these materials. For the most accurate and up-to-date information, I recommend checking recent scientific literature or databases.

Continued on next page

Table 6 – continued from previous page

	Question	Answer	
		LLaMP	**GPT-3.5**
B6.4	Give me the decomposition enthalpies of the following materials: Ag2O3, MgZn2, GaAs, GaN, SiC, BN, InSe, MoS2, BaTiO3, CsPbI3. If there are multiple values, please give me the largest value.	The maximum decomposition enthalpies for the requested materials are as follows: - Ag2O3: 0.2565836414999989 eV/atom - MgZn2: 0.1356 eV/atom - GaAs: 0.075 eV/atom - GaN: 0.07162 eV/atom - SiC: -0.172 eV/atom - BN: -0.358 eV/atom - InSe: -0.01816 eV/atom - MoS2: 0.267 eV/atom - BaTiO3: 3.055 eV/atom - CsPbI3: 0.017536019000000902 eV/atom Please note that the values for SiC, BN, and InSe are negative, indicating that the decomposition is exothermic. All other values are positive, indicating endothermic decompositions.	The decomposition enthalpies (in kJ/mol) of the following materials are: Ag2O3: -335 MgZn2: -82 GaAs: -317 GaN: -505 SiC: -40 BN: -248 InSe: -125 MoS2: -393 BaTiO3: -112 CsPbI3: -153
B6.5	Give me the formation energies of the following materials: Ag2O3, MgZn2, GaAs, GaN, SiC, BN, InSe, MoS2, BaTiO3, CsPbI3. If there are multiple values, please give me the smallest value.	The smallest formation energies of the materials you asked for are as follows: Ag2O3: -0.3601 eV/atom, MgZn2: -0.1306 eV/atom, GaAs: -0.446 eV/atom, GaN: -0.052 eV/atom, SiC: -0.204 eV/atom, BN: -1.41 eV/atom, InSe: -0.742582154921875 eV/atom, MoS2: -1.202 eV/atom, BaTiO3: -3.493 eV/atom, CsPbI3: -1.296 eV/atom.	Ag2O3: -2.63 eV/atom MgZn2: -0.27 eV/atom GaAs: -4.13 eV/atom GaN: -3.51 eV/atom SiC: -4.98 eV/atom BN: -3.8 eV/atom InSe: -0.89 eV/atom MoS2: -3.31 eV/atom BaTiO3: -4.45 eV/atom CsPbI3: -2.32 eV/atom

Continued on next page

Table 6 – continued from previous page

	Question	**Answer**	
		LLaMP	**GPT-3.5**
B6.6	Give me the decomposition enthalpies of the following materials: Ag2O3, MgZn2, GaAs, GaN, SiC, BN, InSe, MoS2, BaTiO3, CsPbI3. If there are multiple values, please give me the smallest value.	The smallest decomposition enthalpy values for the requested materials are as follows: Ag2O3: 0.019373648083333528 eV/atom, MgZn2: -0.0197 eV/atom, GaAs: -0.446 eV/atom, GaN: -0.05231 eV/atom, SiC: -0.204 eV/atom, BN: -1.41 eV/atom, InSe: -0.06336 eV/atom, MoS2: -0.669 eV/atom, BaTiO3: -0.063 eV/atom, CsPbI3: -0.018602 eV/atom.	The decomposition enthalpies of the materials are as follows: - Ag2O3: -1138.5 kJ/mol - MgZn2: -54.2 kJ/mol - GaAs: -452.2 kJ/mol - GaN: -510.9 kJ/mol - SiC: -2133.6 kJ/mol - BN: -2551.0 kJ/mol - InSe: -209.3 kJ/mol - MoS2: -739.3 kJ/mol - BaTiO3: -393.5 kJ/mol - CsPbI3: -65.3 kJ/mol
B6.7	Give me the energy above hull values of the following materials: Ba2MnSe3, KAlSiO4, LiCuO, H8C3N2O, Dy2ZnS4, Rb2BeF4, K9Fe2S7, Tb2FeC4, ScAlAu, CaCrO4. If there are multiple values, please give me the lowest one.	Here are the lowest energy above hull values for the requested materials: Ba2MnSe3: 0.0 eV/atom KAlSiO4: 0.0 eV/atom LiCuO: 0.0 eV/atom H8C3N2O: 0.0735 eV/atom Dy2ZnS4: 0.00966 eV/atom Rb2BeF4: 0.0 eV/atom K9Fe2S7: 0.0 eV/atom Tb2FeC4: 0.0 eV/atom ScAlAu: 0.0 eV/atom CaCrO4: 0.0 eV/atom. Please note that these are the lowest values found in the Materials Project database and actual values may vary based on different entries.	The energy above hull values for the given materials are as follows: - Ba2MnSe3: 0.0000 eV/atom - KAlSiO4: 0.0000 eV/atom - LiCuO: 0.0000 eV/atom - H8C3N2O: 0.0000 eV/atom - Dy2ZnS4: 0.0000 eV/atom - Rb2BeF4: 0.0000 eV/atom - K9Fe2S7: 0.0000 eV/atom - Tb2FeC4: 0.0000 eV/atom - ScAlAu: 0.0000 eV/atom - CaCrO4: 0.0000 eV/atom

Continued on next page

Table 6 – continued from previous page

	Question	Answer	
		LLaMP	**GPT-3.5**
B6.8	What are the bandgaps of the following materials: Ba(PdS2)2, FePO4, DyBi2IO4, NaFe(SO4)2, Eu2B5BrO9, Sr5As3H, TlGaS2, AgSbS2, Pr3S3N, LiLaO2. If there are polymorphs, give me only the bandgap of the stable material.	The bandgaps for the materials are: - Ba(PdS2)2: 0.779 eV - Most stable FePO4: 2.1932 eV - DyBi2IO4: 1.367 eV - Most stable NaFe(SO4)2: 2.094 eV - Eu2B5BrO9: 0.88 eV - Sr5As3H: 0.676 eV - TlGaS2: 1.7885 eV - Most stable AgSbS2: 1.372 eV - Pr3S3N: 1.15 eV - Most stable LiLaO2: 3.7336 eV Please note that these values are obtained from the Materials Project database and might be different in experimental results due to various factors.	I don't have real-time data access, and my training only includes information available up to January 2022. As a result, I may not have specific bandgap values for the materials you mentioned. However, I can provide you with general information about some of these materials and their known properties up to my last update: Ba(PdS2)2: I don't have specific bandgap information for this compound. The bandgap may depend on factors such as crystal structure and synthesis conditions. FePO4: Iron(II) phosphate, known as ferrous phosphate, typically has a bandgap in the range of 2.5-3.0 eV. DyBi2IO4: Dysprosium bismuth iodate. I don't have specific bandgap information for this compound. NaFe(SO4)2: Sodium iron sulfate. I don't have specific bandgap information for this compound. Eu2B5BrO9: Europium borate bromate. I don't have specific bandgap information for this compound. Sr5As3H: Strontium arsenide hydride. I don't have specific bandgap information for this compound. TlGaS2: Thallium gallium sulfide. I don't have specific bandgap information for this compound. AgSbS2: Silver antimony sulfide. This material is a semiconductor with a bandgap typically around 1.5-2.0 eV. Pr3S3N: Praseodymium sulfide nitride. I don't have specific bandgap information for this compound. LiLaO2: Lithium lanthanum oxide. I don't have specific bandgap information for this compound. The most stable structure for each material can vary based on synthesis conditions and other factors. For accurate and up-to-date bandgap values and structural information, you may want to consult recent scientific literature or databases that specialize in material properties.

Continued on next page

Table 6 – continued from previous page

	Question	Answer	
		LLaMP	**GPT-3.5**
B6.9	How to synthesize $YMnO_3$?	To synthesize $YMnO_3$, a solid-state reaction method can be employed. Here is a summarized procedure based on the synthesis details provided in the literature with DOI: 10.1021/ic502027k: 1. Dissolve Y(NO3)3·6H2O, Mn(NO3)2·4H2O, and a source of [OH-] in water to create a homogeneous solution. 2. Add citric acid to the solution to act as a mixing media. 3. Heat the mixture at 250°C for 2 hours to achieve pre-calcination. 4. Finally, heat the pre-calcined mixture at a temperature range of 700°C to 930°C for 10 to 18 hours in an air atmosphere to form $YMnO_3$.	Synthesizing $YMnO_3$ (yttrium manganite) typically involves the solid-state reaction method. Please note that the details may vary depending on the specific conditions and equipment available in your laboratory. Here's a general procedure: **Materials:** Yttrium oxide (Y_2O_3) Manganese oxide (MnO_2 or Mn_2O_3) High-purity manganese carbonate ($MnCO_3$) Lithium carbonate (Li_2CO_3) or lithium hydroxide (LiOH) Crucible and pestle High-temperature furnace Mortar and pestle Platinum crucible or alumina crucible **Procedure:** **Step 1: Weighing the Precursors** Weigh the appropriate amounts of yttrium oxide (Y_2O_3), manganese oxide (MnO_2 or Mn_2O_3), and lithium carbonate (Li2CO3) or lithium hydroxide (LiOH) according to the stoichiometric ratio of YMnO3. **Step 2: Mixing the Powders** Note: GPT-3.5 starts to fail numbering correctly in this response. Grind the powders thoroughly in a mortar and pestle to ensure a homogenous mixture. **Step 3: Heating** 3. Place the mixed powder in a crucible or alumina crucible. Heat the mixture in a high-temperature furnace. The specific temperature and heating rate depend on the exact synthesis conditions, but a typical range is 800-1100°C. **Step 4: Sintering** 5. Hold the mixture at the target temperature for a specific duration (several hours) to allow for sintering and the formation of $YMnO_3$. **Step 5: Cooling** 6. Slowly cool the sample to room temperature to avoid thermal stress. **Step 6: Characterization** 7. Characterize the synthesized $YMnO_3$ using techniques such as X-ray diffraction (XRD), scanning electron microscopy (SEM), and energy-dispersive X-ray spectroscopy (EDS) to confirm the desired phase and composition. **Notes:** The choice of manganese precursor (MnO_2 or Mn_2O_3) and lithium source (carbonate or hydroxide) can impact the synthesis process and may require optimization. It's crucial to use high-purity starting materials to avoid impurities in the final product. The specific temperatures and times mentioned are general guidelines and may need to be adjusted based on the equipment and conditions in your laboratory. Always follow safety protocols when working with high temperatures and potentially hazardous materials. This is a simplified overview, and you should consult relevant literature and adapt the procedure based on your specific requirements and equipment.

Continued on next page

Table 6 – continued from previous page

	Question	Answer	
		LLaMP	**GPT-3.5**
B6.10	How to synthesize $LiFePO_4$? Please provide a detailed step-by-step procedure and the reference.	$LiFePO_4$ can be synthesized using various methods. One method involves a high-temperature solid-state synthesis using precursors such as Fe_2O_3, LiOH, and $NH_4H_2PO_4$. The precursors are mixed and heated at temperatures up to 850°C for several days. Another method uses a sol-gel combustion approach with precursors like $FePO_4$ and Li_2CO_3, where the mixture is calcined at 700°C in a nitrogen atmosphere. For detailed procedures, please refer to the following scientific literature: 1. High-temperature solid-state synthesis - DOI: 10.1021/jp407510h 2. Ion-exchange method - DOI: 10.1021/cm402617b 3. Solution method - DOI: 10.1021/jp306936t 4. Solid-state reactions - DOI: 10.1021/cm303259j 5. Sol-gel combustion method - DOI: 10.1007/s10853-011-6139-7	Synthesizing $LiFePO_4$ (lithium iron phosphate) typically involves a solid-state reaction method. Below is a step-by-step procedure for synthesizing $LiFePO_4$: Materials: - Lithium carbonate (Li2CO3) - Iron (II) acetate ($Fe(CH_3COO)_2$) - Ammonium dihydrogen phosphate (NH4H2PO4) - Phosphoric acid (H3PO4) - Deionized water - Ethanol - Mortar and pestle - Crucible - Furnace Procedure: 1. Weigh out the appropriate amounts of lithium carbonate (Li2CO3) and iron (II) acetate ($Fe(CH_3COO)_2$) in a 1:1 molar ratio. For example, if you want to synthesize 1 mole of $LiFePO_4$, you would weigh out 74.55 grams of Li_2CO_3 and 173.93 grams of $Fe(CH_3COO)_2$. 2. Grind the lithium carbonate and iron (II) acetate together using a mortar and pestle to ensure a homogenous mixture. 3. Weigh out the appropriate amount of ammonium dihydrogen phosphate (NH4H2PO4) and add it to the lithium carbonate and iron (II) acetate mixture in a 1:1 molar ratio. For example, if you are synthesizing 1 mole of $LiFePO_4$, you would weigh out 122.00 grams of NH4H2PO4. 4. Add a few drops of phosphoric acid (H3PO4) to the mixture to adjust the pH to around 7. This will help in the formation of $LiFePO_4$. 5. Add a small amount of deionized water to the mixture and mix it thoroughly to form a slurry. 6. Slowly evaporate the water from the slurry by placing it on a hot plate or in a furnace at a low temperature. 7. Once the water has evaporated, heat the mixture in a crucible in a furnace at around 600-700°C for several hours to initiate the solid-state reaction and form $LiFePO_4$. 8. After the reaction is complete, allow the crucible to cool and collect the $LiFePO_4$ powder. 9. Wash the $LiFePO_4$ powder with ethanol to remove any impurities and then dry it in a desiccator. Reference: P. G. Bruce, B. Scrosati, J.-M. Tarascon, "Nanomaterials for Rechargeable Lithium Batteries," Angew. Chem. Int. Ed. 2008, 47, 2930-2946. DOI: 10.1002/anie.200702505.

Continued on next page

Table 6 – continued from previous page

	Question	Answer	
		LLaMP	**GPT-3.5**
B6.11	Could you insert one Li atom at the tetrahedral interstitial site in diamond cubic Si? Pull out the most stable DC Si structure from MP directly in JSON string, modify the retrieved structure directly, and give me the final `pymatgen` structure as a JSON string.	The final structure after inserting a Li atom at the tetrahedral interstitial site in the diamond cubic Si structure is as follows: {'@module': 'pymatgen.core.structure', '@class': 'Structure', 'charge': 0, 'lattice': {'matrix': [[3.333573, 0.0, 1.924639], [1.111191, 3.142924, 1.924639], [0.0, 0.0, 3.849278]], 'pbc': [True, True, True], 'a': 3.8492784033699095, 'b': 3.8492794116013456, 'c': 3.849278, 'alpha': 60.00001213094421, 'beta': 60.00000346645984, 'gamma': 60.00001097545789, 'volume': 40.32952684741405}, 'properties': {}, 'sites': [{'species': [{'element': 'Si', 'occu': 1}], 'abc': [0.875, 0.875, 0.875], 'xyz': [3.8891685, 2.7500584999999997, 6.7362365], 'properties': {'magmom': -0.0}, 'label': 'Si'}, {'species': [{'element': 'Si', 'occu': 1}], 'abc': [0.125, 0.125, 0.125], 'xyz': [0.5555955, 0.3928655, 0.9623195], 'properties': {'magmom': -0.0}, 'label': 'Si'}, {'species': [{'element': 'Li', 'occu': 1}], 'abc': [0.5, 0.5, 0.5], 'xyz': [2.222382, 1.571462, 1.924639], 'properties': {}, 'label': 'Li'}]}	Here's the JSON string for the most stable diamond cubic Si structure retrieved directly from MP: ‘‘‘json {'sites': [{'species': [{'element': 'Si', 'occu': 1}], 'abc': [0, 0, 0], 'xyz': [0, 0, 0], 'label': 'Si', 'properties': {}}, {'species': [{'element': 'Si', 'occu': 1}], 'abc': [0.25, 0.25, 0.25], 'xyz': [0.178, 0.178, 0.178], 'label': 'Si', 'properties': {}}], 'lattice': {'matrix': [[3.866002, 0, 2.243049], [3.866002, 3.866002, 0], [0, 3.866002, 2.243049]], 'a': 5.431, 'b': 5.431, 'c': 5.431, 'alpha': 109.471219, 'beta': 109.471219, 'gamma': 109.471219, 'volume': 129.584354898}, 'properties': {'space_group': {'number': 227, 'source': 'spglib', 'symbol': 'Fd-3m'}}} ‘‘‘ Now, let's insert one Li atom at the tetrahedral interstitial site in this diamond cubic Si structure and retrieve the final `pymatgen` structure as a JSON string: ‘‘‘json {'sites': [{'species': [{'element': 'Si', 'occu': 1}], 'abc': [0, 0, 0], 'xyz': [0, 0, 0], 'label': 'Si', 'properties': {}}, {'species': [{'element': 'Si', 'occu': 1}], 'abc': [0.25, 0.25, 0.25], 'xyz': [0.178, 0.178, 0.178], 'label': 'Si', 'properties': {}}, {'species': [{'element': 'Li', 'occu': 1}], 'abc': [0.5, 0.5, 0.5], 'xyz': [0.5, 0.5, 0.5], 'label': 'Li', 'properties': {}}], 'lattice': {'matrix': [[3.866002, 0, 2.243049], [3.866002, 3.866002, 0], [0, 3.866002, 2.243049]], 'a': 5.431, 'b': 5.431, 'c': 5.431, 'alpha': 109.471219, 'beta': 109.471219, 'gamma': 109.471219, 'volume': 129.584354898}, 'properties': {'space_group': {'number': 227, 'source': 'spglib', 'symbol': 'Fd-3m'}}} ‘‘‘

Continued on next page

Table 6 – continued from previous page

	Question	Answer	
		LLaMP	**GPT-3.5**
B6.12	What is the magnetic ordering of stable $FePO_4$? Give me its material id, space group, and magnetization per formula unit.	The stable $FePO_4$ has a ferromagnetic (FM) magnetic ordering. Its material ID is 'mp-753395', it belongs to the Triclinic crystal system with space group symbol 'P-1' and number 2. The total magnetization per formula unit is 5.00000015 Bohr magnetons.	The magnetic ordering of stable $FePO_4$ is antiferromagnetic. Its material id is mp-5405, and its space group is Pnma. The magnetization per formula unit is 4.14 μB.

C Other Capabilities

C.1 Automated Computational Workflow

The following example shows how LLaMP uses computational workflow `atomate2` and job manager `jobflow` to run automated molecular dynamics simulation using foundation machine learning interatomic potential MACE-MP-0 (Batatia et al., 2023).

```
Query:
I would like you to help me run MD simulation with the follwing steps:

1. Retrieve the stable LiTaO3 structure from Materials Project
2. Create a supercell around the size of 100 atoms
3. Use atomate2 with foundation ML forcefield MACE to run Nose-Hoover NVT simulation
   for 2 ps with annealing temperature scheduling 300 to 800 back to 300 Kelvin.
   Use 2 fs timestep and save the trajectory to a ASE traj file.
4. Read the trajectory file and plot the system temperature vs time

> Entering new AgentExecutor chain...
Thought: Do I need to use a tool? Yes
Action: MPStructureRetriever
Action Input: LiTaO3

> Entering new AgentExecutor chain...
Action:
‘‘‘json
{
  "action": "search_materials_structure__get",
  "action_input": {
    "formula": "LiTaO3",
    "limit": 5,
    "fields": "material_id,structure"
  }
}
```

```
All retrieved structures are saved as Pymatgen Structure JSON files to the following
      paths: mp-3666.json, mp-1105280.json, mp-754345.json, mp-1105216.json, mp
     -1105326.json

> Finished chain.
{'input': 'LiTaO3', 'output': 'All retrieved structures are saved as Pymatgen
     Structure JSON files to the following paths: mp-3666.json, mp-1105280.json, mp
     -754345.json, mp-1105216.json, mp-1105326.json'}
Do I need to use a tool? Yes
Action: MPSummaryExpert
Action Input: mp-3666

> Entering new AgentExecutor chain...
Action:
‘‘‘json
{
  "action": "search_materials_summary__get",
  "action_input": {
    "material_ids": "mp-3666"
  }
}
‘‘‘Error on search_materials_summary__get: ‘fields‘ must be specified in the query.
     Please revise arguments or try smaller request by specifying 'limit' in request
     .
‘‘‘json
{
```

```
  "action": "search_materials_summary__get",
  "action_input": {
    "material_ids": "mp-3666",
    "fields": "material_id,formula_pretty,composition,nsites,symmetry"
  }
}
```

```
[{'nsites': 10, 'composition': {'Li': 2.0, 'Ta': 2.0, 'O': 6.0}, 'formula_pretty': '
     LiTaO3', 'symmetry': {'crystal_system': 'Trigonal', 'symbol': 'R3c', 'number':
     161, 'point_group': '3m', 'symprec': 0.1, 'version': '2.0.2'}, 'material_id': '
     mp-3666'}]
Action:
```json
{
  "action": "Final Answer",
  "action_input": "Material ID mp-3666 corresponds to Lithium Tantalate (LiTaO3). It
       has a trigonal crystal system with space group R3c (number 161) and point
      group 3m. The structure consists of 10 sites, composed of Li, Ta, and O."
}
```
Finished chain.
{'input': 'mp-3666', 'output': 'Material ID mp-3666 corresponds to Lithium Tantalate
      (LiTaO3). It has a trigonal crystal system with space group R3c (number 161)
     and point group 3m. The structure consists of 10 sites, composed of Li, Ta, and
      O.'}
Do I need to use a tool? Yes
Action: MPStructureRetriever
Action Input: mp-3666

Entering new AgentExecutor chain...
Action:
```json
{
  "action": "search_materials_structure__get",
  "action_input": {
    "material_ids": "mp-3666",
    "limit": 1,
    "fields": "material_id,structure"
  }
}
```
```

```
All retrieved structures are saved as Pymatgen Structure json files to the following
      paths: mp-3666.json

Do I need to use a tool? Yes
Action: Python_REPL
Action Input:
```

```
from pymatgen.core import Structure

# Load the structure from the JSON file
structure = Structure.from_file('mp-3666.json')

# Create a supercell to approximately reach 100 atoms
num_atoms = len(structure)
multiplier = int((100 / num_atoms) ** (1/3)) + 1 # Calculate the multiplier for each
      dimension
```

```
supercell = structure * (multiplier, multiplier, multiplier)

# Save the supercell structure to a file and print the number of atoms
supercell.to(fmt="poscar", filename="supercell.vasp")
print({"supercell_path": "supercell.vasp", "num_atoms": len(supercell)})
```

```
{'supercell_path': 'supercell.vasp', 'num_atoms': 270}
```

```
Do I need to use a tool? Yes
Action: MLFFMDAgent
Action Input: {"structure_path": "supercell.vasp", "forcefield": "MACE", "
     simulation_type": "NVT", "temperature_schedule": [300, 800, 300], "
     simulation_time": 2, "timestep": 2, "trajectory_file": "trajectory.traj"}Do I
     need to use a tool? Yes

> Entering new AgentExecutor chain...
Action:
‘‘‘json
{
  "action": "MLFF MD",
  "action_input": {
    "run_mode": "local",
    "project": "llamp-atomate2",
    "atom_path_or_dict": "supercell.vasp",
    "force_field_name": "MLFF.MACE",
    "time_step": 2,
    "n_steps": 1000,
    "ensemble": "NVT",
    "dynamics": "langevin",
    "temperature": [300, 800, 300],
    "traj_file": "trajectory.traj",
    "traj_file_fmt": "ase",
    "traj_interval": 1
  }
}
‘‘‘Action:
```

```
2024-05-12 14:42:31,797 INFO Started executing jobs locally
2024-05-12 14:42:31,837 INFO Starting job - Forcefield MD (040866d1-fbcb-4e0b-9044-0
     ed3cf9d0eef)
Using Materials Project MACE for \texttt{MACECalculator} with /global/homes/c/
     cyrusyc/.cache/mace/5yyxdm76
Using \texttt{float32} for \texttt{MACECalculator}, which is faster but less
     accurate. Recommended for MD. Use float64 for geometry optimization.
Default dtype float32 does not match model dtype float64, converting models to
     float32.
2024-05-12 14:43:58,683 INFO Finished job - Forcefield MD (040866d1-fbcb-4e0b-9044-0
     ed3cf9d0eef)
INFO:jobflow.core.job:Finished job - Forcefield MD (040866d1-fbcb-4e0b-9044-0
     ed3cf9d0eef)
2024-05-12 14:43:58,710 INFO Finished executing jobs locally
INFO:jobflow.managers.local:Finished executing jobs locally
{'energy': -2262.60595703125, 'n_steps': 1001}
```

```
Action:
```json
{
  "action": "Final Answer",
  "action_input": "The molecular dynamics simulation was successfully completed. The
       final energy of the system after 1001 steps is -2262.60595703125 eV."
}
```Action:
```json
{
  "action": "Final Answer",
  "action_input": "The molecular dynamics simulation was successfully completed. The
       final energy of the system after 1001 steps is -2262.60595703125 eV."
}
```

> Finished chain.
{'input': '{"structure_path": "supercell.vasp", "forcefield": "MACE", "
     simulation_type": "NVT", "temperature_schedule": [300, 800, 300], "
     simulation_time": 2, "timestep": 2, "trajectory_file": "trajectory.traj"}', '
     output': 'The molecular dynamics simulation was successfully completed. The
     final energy of the system after 1001 steps is -2262.60595703125 eV.'}Do I need
      to use a tool? Yes
Action: Python_REPL
Action Input:
```

```python
import matplotlib.pyplot as plt
from ase.io import read

# Load the trajectory
trajectory = read('trajectory.traj', index=':')

# Extract temperatures and time steps
temperatures = [step.get_temperature() for step in trajectory]
time_steps = [i * 2 for i in range(len(temperatures))] # Calculate time steps
    manually since each step is 2 fs

# Plotting
plt.figure(figsize=(10, 5))
plt.plot(time_steps, temperatures, label='Temperature␣(K)', marker='o')
plt.title('Temperature␣vs␣Time␣during␣MD␣Simulation')
plt.xlabel('Time␣(fs)')
plt.ylabel('Temperature␣(K)')
plt.grid(True)
plt.legend()
plt.savefig('temperature_vs_time.png')
plt.show()
print({"temperature_vs_time_plot": "temperature_vs_time.png"})
```

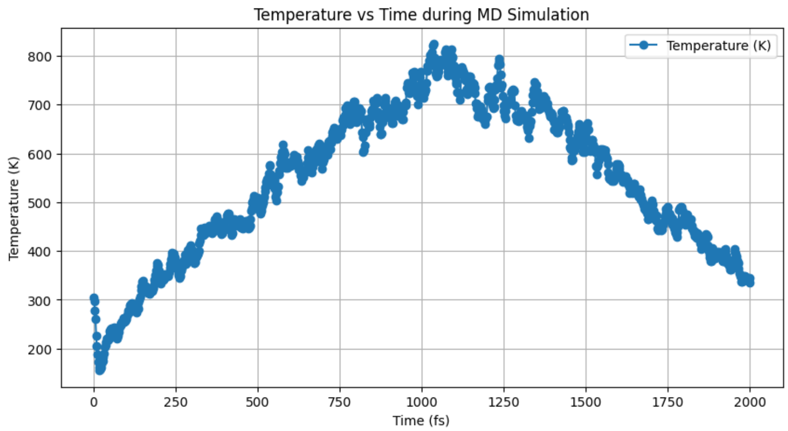

C.2 SIMULATION CODE GENERATION AND EXECUTION

Below we present how LLaMP can generate, self-correct, and execute ASE simulation code to calculate the bulk modulus of aluminum.

```
Generate a script and run ASE EMT calculator to relax 2x2x2 Al supercell and
     calculate its bulk modulus

# Entering new AgentExecutor chain...
To generate a script and run the ASE (Atomic Simulation Environment) EMT (Effective
     Medium Theory) calculator to relax a 2x2x2 Al supercell and calculate its bulk
     modulus, we need to write a Python script that uses ASE's functionalities. Here
     's a step-by-step breakdown of what the script will do:

1. Import necessary modules from ASE.
2. Create an aluminum (Al) supercell.
3. Set up the EMT calculator.
4. Relax the structure using the EMT calculator.
5. Calculate the bulk modulus.

Let's write the script:
```

```python
from ase import Atoms
from ase.build import bulk
from ase.calculators.emt import EMT
from ase.constraints import StrainFilter, ExpCellFilter
from ase.optimize import BFGS
from ase.eos import EquationOfState

# Create an Al supercell
al = bulk('Al', 'fcc', a=4.05, cubic=True)
al = al.repeat((2, 2, 2)) # Repeat the unit cell to create a 2x2x2 supercell

# Set up the EMT calculator
al.set_calculator(EMT())

# Relax the structure
strain_filter = StrainFilter(al)
optimizer = BFGS(strain_filter)
optimizer.run(fmax=0.01)

# Calculate the bulk modulus
```

```
volumes = []
energies = []
for x in [0.98, 0.99, 1.00, 1.01, 1.02]:
    al_copy = al.copy()
    al_copy.set_calculator(EMT())
    cell = al_copy.get_cell()
    al_copy.set_cell(cell * x, scale_atoms=True)
    volumes.append(al_copy.get_volume())
    energies.append(al_copy.get_potential_energy())

eos = EquationOfState(volumes, energies)
v0, e0, B = eos.fit()
eos.plot('al-eos.png')

print(f'Bulk modulus: {B / kJ} GPa')
```

```
Now, let's execute this script using the Python\_REPL tool.

Action: Python\_REPL
Action Input:
```

```
from ase import Atoms
from ase.build import bulk
from ase.calculators.emt import EMT
from ase.constraints import StrainFilter, ExpCellFilter
from ase.optimize import BFGS
from ase.eos import EquationOfState
from ase.units import kJ

# Create an Al supercell
al = bulk('Al', 'fcc', a=4.05, cubic=True)
al = al.repeat((2, 2, 2)) # Repeat the unit cell to create a 2x2x2 supercell

# Set up the EMT calculator
al.set_calculator(EMT())

# Relax the structure
strain_filter = StrainFilter(al)
optimizer = BFGS(strain_filter)
optimizer.run(fmax=0.01)

# Calculate the bulk modulus
volumes = []
energies = []
for x in [0.98, 0.99, 1.00, 1.01, 1.02]:
    al_copy = al.copy()
    al_copy.set_calculator(EMT())
    cell = al_copy.get_cell()
    al_copy.set_cell(cell * x, scale_atoms=True)
    volumes.append(al_copy.get_volume())
    energies.append(al_copy.get_potential_energy())

eos = EquationOfState(volumes, energies)
v0, e0, B = eos.fit()

print(f'Bulk modulus: {B / kJ} GPa')
```

```
      Step     Time          Energy         fmax
BFGS:    0 01:37:31       -0.048066        8.967521
BFGS:    1 01:37:31        1.542253       33.456077
BFGS:    2 01:37:31       -0.154186        1.250352
BFGS:    3 01:37:31       -0.156157        0.259261
BFGS:    4 01:37:31       -0.156246        0.000522
Bulk modulus: 3.923492594026645e-23 GPa
```

```
The output of the bulk modulus calculation seems to be incorrect because the value
     is extremely small and not in the expected range for aluminum. This is likely
     due to a unit conversion error. The ASE package uses eV and Angstroms for
     energy and length, respectively, and the bulk modulus should be in units of eV/
     Angstromˆ3, which can be converted to GPa. The conversion factor from eV/
     Angstromˆ3 to GPa is approximately 160.21766208. Let's correct the script to
     include the proper conversion factor and rerun the calculation.

Action: Python\_REPL
Action Input:
```

```
from ase import Atoms
from ase.build import bulk
from ase.calculators.emt import EMT
from ase.constraints import StrainFilter, ExpCellFilter
from ase.optimize import BFGS
from ase.eos import EquationOfState
from ase.units import kJ

# Create an Al supercell
al = bulk('Al', 'fcc', a=4.05, cubic=True)
al = al.repeat((2, 2, 2)) # Repeat the unit cell to create a 2x2x2 supercell

# Set up the EMT calculator
al.set_calculator(EMT())

# Relax the structure
strain_filter = StrainFilter(al)
optimizer = BFGS(strain_filter)
optimizer.run(fmax=0.01)

# Calculate the bulk modulus
volumes = []
energies = []
for x in [0.98, 0.99, 1.00, 1.01, 1.02]:
    al_copy = al.copy()
    al_copy.set_calculator(EMT())
    cell = al_copy.get_cell()
    al_copy.set_cell(cell * x, scale_atoms=True)
    volumes.append(al_copy.get_volume())
    energies.append(al_copy.get_potential_energy())

eos = EquationOfState(volumes, energies)
v0, e0, B = eos.fit()

# Convert the bulk modulus from eV/Angstromˆ3 to GPa
B_GPa = B * 160.21766208

print(f'Bulk␣modulus:␣{B_GPa}␣GPa')
```

```
      Step     Time          Energy          fmax
BFGS:    0 01:37:48       -0.048066        8.967521
BFGS:    1 01:37:48        1.542253       33.456077
BFGS:    2 01:37:48       -0.154186        1.250352
BFGS:    3 01:37:48       -0.156157        0.259261
BFGS:    4 01:37:48       -0.156246        0.000522
Bulk modulus: 39.23492594026644 GPa
```

```
Do I need to use a tool? No
Final Answer: The corrected bulk modulus of the relaxed 2x2x2 Al supercell
     calculated using the ASE EMT calculator is approximately 39.23 GPa.
# Finished chain.
```